U.S. DEPARTMENT OF ENERGY | National Energy Technology Laboratory

OFFICE OF FOSSIL ENERGY

Analysis of Brayton Cycles Utilizing Supercritical Carbon Dioxide

July 1, 2014

DOE/NETL-4001/070114

Disclaimer

This report was prepared as an account of work sponsored by an agency of the United States Government. Neither the United States Government nor any agency thereof, nor any of their employees, makes any warranty, express or implied, or assumes any legal liability or responsibility for the accuracy, completeness, or usefulness of any information, apparatus, product, or process disclosed, or represents that its use would not infringe privately owned rights. Reference therein to any specific commercial product, process, or service by trade name, trademark, manufacturer, or otherwise does not necessarily constitute or imply its endorsement, recommendation, or favoring by the United States Government or any agency thereof. The views and opinions of authors expressed therein do not necessarily state or reflect those of the United States Government or any agency thereof.

All exhibits have been created by the National Energy Technology Laboratory, unless otherwise noted.

Author List:

Energy Sector Planning and Analysis (ESPA)

Charles White
Noblis

This report was prepared by Energy Sector Planning and Analysis (ESPA) for the United States Department of Energy (DOE), National Energy Technology Laboratory (NETL). This work was completed under DOE NETL Contract Number DE-FE0004001. This work was performed under ESPA Task 341.03.04.

The authors wish to acknowledge the excellent guidance, contributions, and cooperation of the NETL staff, particularly:

Walter Shelton, NETL Technical Monitor

Kristin Gerdes, Director of Office of Program Performance & Benefits

Richard Dennis, Technology Manager for Turbines

DOE Contract Number DE-FE0004001

This page intentionally left blank.

Table of Contents

Executive Summary 1
1 Introduction 4
2 Non-recuperated Brayton Cycle 5
2.1 Aspen Plus® Simulations of Simple Non-recuperated Brayton Cycle 6
2.2 Impact of Working Fluid 12
2.3 Impact of Turbine Inlet Temperature 13
2.4 Impact of Turbine and Compressor Efficiency 16
2.5 Impact of Turbine Exit Pressure 21
3 CO_2 Physical Properties 23
4 Recuperated Brayton Cycle 27
4.1 Impact of Pressure Ratio 28
4.2 Analysis of Recuperation 29
4.3 Impact of Working Fluid 31
4.4 Impact of Turbine Inlet Temperature 31
4.5 Impact of Turbine and Compressor Efficiency 32
4.6 Impact of Turbine Exit Pressure 33
5 Two-stage Recuperated (Recompression) Brayton Cycle 37
5.1 Impact on Recuperator Effectiveness 38
5.2 Impact of Pressure Ratio 40
5.3 Impact of Turbine Inlet Temperature 40
5.4 Impact of Turbine and Compressor Efficiency 41
5.5 Impact of Turbine Exit Pressure 42
5.6 Impact of Working Fluid 45
6 Recompression Brayton Cycle with Reheat 46
6.1 Impact of Pressure Ratio 46
6.2 Impact of Turbine and Compressor Efficiency 47
7 Conclusions 50
8 Recommendations 52
9 References 53

Exhibits

Exhibit 2-1 Simple Brayton cycle without recuperation 5
Exhibit 2-2 Parameters used in Aspen Plus® simulations 6
Exhibit 2-3 Efficiency versus pressure ratio for a simple Brayton cycle with sCO_2 and 1300 °F TIT 7
Exhibit 2-4 Impact of TIT on efficiency versus pressure ratio for a simple Brayton cycle with sCO_2 7
Exhibit 2-5 Efficiency versus pressure ratio for a simple Brayton cycle with sCO_2 and 1300 °F TIT 8
Exhibit 2-6 Specific power versus pressure ratio for a simple Brayton cycle with sCO_2 and 1300 °F TIT 9
Exhibit 2-7 Specific power versus pressure ratio for a simple Brayton cycle with sCO_2 and 1300 °F and 1800 °F TIT 10
Exhibit 2-8 Simple Brayton cycle with sCO_2 and 1300 °F TIT, turbine and compressor exit temperatures 11
Exhibit 2-9 Simple Brayton cycle with sCO_2 and 1800 °F TIT, turbine and compressor exit temperatures 11
Exhibit 2-10 Cycle efficiency as a function of pressure ratio 12
Exhibit 2-11 Specific power as a function of pressure ratio 13
Exhibit 2-12 Cycle efficiency versus pressure ratio at different TIT 13
Exhibit 2-13 CO_2 Brayton cycle efficiency versus turbine inlet temperature 14
Exhibit 2-14 N_2 Brayton cycle efficiency versus turbine inlet temperature 15
Exhibit 2-15 Brayton cycle-specific power dependence on turbine inlet temperature 15
Exhibit 2-16 Brayton cycle efficiency dependence on turbine isentropic efficiency 16
Exhibit 2-17 Brayton cycle-specific power dependence on turbine isentropic efficiency 17
Exhibit 2-18 Brayton cycle efficiency dependence on compressor isentropic efficiency 18
Exhibit 2-19 Brayton cycle-specific power dependence on compressor isentropic efficiency 19
Exhibit 2-20 Brayton cycle efficiency dependence on turbine and compressor isentropic efficiency 20
Exhibit 2-21 Brayton cycle-specific power dependence on turbine and compressor isentropic efficiency 20
Exhibit 2-22 Parameters used in Aspen Plus® simulations 21
Exhibit 2-23 Brayton cycle efficiency dependence on turbine exit pressure (psia) 22
Exhibit 2-24 Maximum Brayton cycle efficiency dependence on turbine exit pressure 22
Exhibit 3-1 CO_2 density versus temperature, pressure (psia) 23
Exhibit 3-2 CO_2 c_p versus temperature, pressure (psia) 24
Exhibit 3-3 CO_2 c_p/c_v versus temperature, pressure (psia) 24
Exhibit 3-4 CO_2 density versus temperature, pressure (psia) 25
Exhibit 3-5 CO_2 c_p versus temperature, pressure (psia) 26
Exhibit 3-6 CO_2 c_p/c_v versus temperature, pressure (psia) 26
Exhibit 4-1 Simple Brayton cycle with recuperation 27
Exhibit 4-2 Parameters used in Aspen Plus® simulations for recuperated cycle 28
Exhibit 4-3 Cycle efficiency versus pressure ratio for Brayton cycles with CO_2 28
Exhibit 4-4 Cycle specific power versus pressure ratio for Brayton cycles with CO_2 29
Exhibit 4-5 Heat duties versus pressure ratio for recuperated Brayton CO_2 cycle 30

Exhibit 4-6 Heat duties versus pressure ratio for recuperated Brayton CO_2 cycle..... 30
Exhibit 4-7 Cycle efficiency versus pressure ratio for Brayton cycles with CO_2, N_2, and Ar..... 31
Exhibit 4-8 Impact of turbine inlet temperature for a recuperated Brayton CO_2 cycle..... 32
Exhibit 4-9 Brayton cycle efficiency dependence on turbine and compressor isentropic efficiency 33
Exhibit 4-10 Parameters used in Aspen Plus® simulations..... 34
Exhibit 4-11 Recuperated Brayton cycle efficiency dependence on turbine exit pressure (psia) 34
Exhibit 4-12 Recuperator effectiveness as a function of pressure ratio..... 35
Exhibit 4-13 Recuperated Brayton cycle-specific power dependence on turbine exit pressure... 36
Exhibit 5-1 Two-stage recuperated (recompression) Brayton cycle..... 37
Exhibit 5-2 Temperature-enthalpy diagram for the recuperated Brayton cycle 38
Exhibit 5-3 Temperature-enthalpy diagram for the recompression Brayton cycle, bypass = 0.37 39
Exhibit 5-4 CO_2 recompression Brayton cycle efficiency versus cooler bypass fraction..... 39
Exhibit 5-5 Impact of cycle pressure ratio on the recompression Brayton cycle efficiency 40
Exhibit 5-6 Impact of turbine inlet temperature for a recuperated Brayton CO_2 cycle..... 41
Exhibit 5-7 Impact of turbine and compressor efficiency on recompression Brayton cycle efficiency..... 42
Exhibit 5-8 Recompression Brayton cycle efficiency dependence on turbine exit pressure (psia) 43
Exhibit 5-9 Maximum recompression Brayton cycle efficiency versus turbine exit pressure 44
Exhibit 5-10 Recompression Brayton cycle-specific power dependence on turbine exit pressure 44
Exhibit 5-11 Recompression Brayton cycle efficiency versus pressure ratio for N_2 and Ar 45
Exhibit 6-1 Two-stage recuperated (recompression) Brayton cycle with reheat..... 46
Exhibit 6-2 Cycle efficiency versus pressure ratio for the recompression reheat Brayton cycle . 47
Exhibit 6-3 Impact of turbine and compressor efficiency on recompression reheat Brayton cycle efficiency..... 48
Exhibit 6-4 Recompression reheat Brayton cycle-specific power dependence on pressure ratio 49

Acronyms and Abbreviations

Ar	Argon
atm	Atmosphere (14.696 psi)
BFD	Block flow diagram
Btu	British thermal unit
Btu/hr	British thermal units per hour
CO_2	Carbon dioxide
c_p	Heat capacity at constant pressure
Cseff	Compressor isentropic efficiency
cuft	Cubit foot
c_v	Heat capacity at constant volume
DOE	Department of Energy
ESPA	Energy Sector Planning and Analysis
FE	Fossil energy
h, hr	Hour
hr	Hour
lb	Pound
lb/hr	Pounds per hour
lbmol	Pound mole
lbmole	Pound mole
MM	Million
MMBtu	Million British thermal units
MMBtu/hr	Million British thermal units per hour
MPa	Megapascal
N_2	Nitrogen
NETL	National Energy Technology Laboratory
Pex	Turbine exit pressure
PFBC	Pressurized fluidized bed combustor
PR	Pressure ratio
PR-BM	Peng-Robinson equation of state with Boston-Mathias corrections
psia	Pound per square inch absolute
Q_C	Heat duty for cooler
Q_H	Heat input from hot source
Q_R	Heat duty for recuperator
R&D	Research and development
RB	Recuperated Brayton cycle
REFPROP	National Institute of Standards equation of state
SB	Simple non-recuperated Brayton cycle
SC	Supercritical
sCO_2	Supercritical carbon dioxide
T	Temperature
Ta	Compressor inlet temperature
TIT	Turbine inlet temperature
Tseff	Turbine isentropic efficiency
USC	Ultra-supercritical
w	Specific power (W/lb/hr)
W	Watt
Wc	Compressor power
We	Expander power
γ	c_p/c_v
η	Efficiency
°C	Degrees Celsius
°F	Degrees Fahrenheit
°R	Degrees Rankine

Executive Summary

This white paper documents a detailed and extensive Brayton cycle analysis that was performed to better understand at a fundamental level the dependence of the Brayton cycle performance on operating conditions, working fluid, supercritical fluid properties, and some cycle non-idealities. This work was performed to better understand the factors controlling Brayton cycle performance and optimal operating conditions, particularly for cycles utilizing supercritical CO_2 (sCO_2) as the working fluid.

The focus of this study is on cycle performance, particularly efficiency. No cost estimates were performed. However, as a single indirect measure of cycle cost, some sensitivity analyses on specific power (net output divided by working fluid mass flow rate) were included.

The non-recuperated Brayton cycle is the simplest form of the closed Brayton cycle. For ideal conditions (adiabatic operation, turbo-machinery efficiencies of 1, and no pressure drops), the cycle efficiency increases monotonically with pressure ratio and shows no dependence on turbine inlet temperature. For non-ideal cycles and working fluids, the cycle efficiency increases with turbine inlet temperature and, at any given turbine inlet temperature, shows a maximum at some pressure ratio. The cycle efficiency decreases as either the turbine efficiency or compressor efficiency decreases but the impacts of drops in the turbine efficiency are more significant. The cycle-specific power dependence on pressure ratio shows a maximum that occurs at a lower pressure ratio than the cycle efficiency maximum. The cycle efficiency is greatest for working fluids with the largest value of γ. However, the specific power is greatest for the working fluids with the greatest density and this favors CO_2 when the cycle conditions are such that CO_2 exhibits properties of a supercritical fluid. For the CO_2 Brayton cycle, the cycle efficiency is dependent on cycle pressure. This can best be seen by the sensitivity of cycle efficiency to the turbine exit pressure, which is the minimum cycle pressure if pressure drops are not considered. For the CO_2 Brayton cycle, a maximum in efficiency occurs at a turbine exit pressure of approximately 1200 psia, which is just above the CO_2 critical pressure.

Near the critical region, the physical properties of CO_2 are highly non-ideal and highly non-linear. Variations in c_p, γ, and density are very large in this region and it is essential that the equation of state used to estimate the physical properties of the working fluid capture this behavior to accurately estimate cycle performance. In this work, it was found that the Peng-Robinson equation of state with Boston-Mathias corrections (PR-BM) in Aspen Plus® was able to estimate the properties of CO_2 to an acceptable level of accuracy.

Introducing a recuperator in the Brayton cycle, in which a portion of the sensible heat in the turbine exhaust is used to preheat the working fluid prior to entering the hot source, increases the cycle efficiency at every pressure ratio for which recuperation is feasible. The recuperated Brayton cycle shows a maximum in cycle efficiency that occurs at a much lower pressure ratio than for a non-recuperated cycle. Recuperation acts to increase cycle efficiency by sparing the hot source heat duty and allowing more working fluid to enter the cycle. For an ideal cycle, recuperation has no impact on specific power. In the non-recuperated Brayton cycle, efficiency is not dependent on turbine inlet temperature but there is a strong dependence on turbine inlet temperature seen in the recuperated Brayton cycle. As in the non-recuperated cycle, the cycle efficiency in a recuperated cycle decreases with decreases in turbo-machinery efficiencies but this drop is significantly less in the recuperated Brayton cycle. The efficiency of the recuperated Brayton cycle is strongly dependent on the recuperator effectiveness. The greater the

effectiveness, the less heat is required to attain the turbine inlet temperature and the more working fluid, hence more net output, will result. For ideal fluids, the recuperator effectiveness depends only on pressure ratio, but for CO_2, there is a strong dependence on system pressure as well, due to the large increase in c_p in the region of the critical point. Because of this, the recuperated Brayton cycle dependence on turbine exit pressure is complex and the maximum cycle efficiencies occur at low system pressures. However, the specific power for low system pressures is probably too low for this to be a desired operating point.

The adverse effect of low recuperator effectiveness (when the CO_2 recuperated Brayton cycle operates near the critical point at the compressor entrance) can be ameliorated by the use of the two-stage recompression cycle configuration. Here, a portion of the low pressure CO_2 exiting the recuperator bypasses the CO_2 cooler and enters a second compressor directly. Only the CO_2 that has been cooled enters the low temperature recuperator stage on the cold-side. The cold-side exit stream from the low temperature recuperator stage mixes with the bypassed CO_2 and the combined stream becomes the cold-side fluid for the high temperature recuperator stage. This bypass action lowers the thermal capacitance of the cold-side fluid to be closer to the thermal capacitance of the hot-side fluid, increasing recuperator effectiveness. Although this results in an increase in the compressor work, this is compensated for by the benefits of greater recuperation and greater net cycle output. The recompression configuration boosts efficiency of the recuperated CO_2 cycle, particularly at low pressure ratios where the maximum cycle efficiency occurs. As with the non-recuperated Brayton cycle, the recompression CO_2 Brayton cycle efficiency has a maximum in cycle efficiency at a turbine exit pressure just above the critical pressure. However, it is unclear if the most desired operating state for this cycle occurs at the point of maximum cycle efficiency as the specific power is quite low in this region.

The use of reheat in the recompression Brayton cycle yields an increase in both cycle efficiency and specific power although this increase is greatest at large pressure ratios. Reheat also decreases the sensitivity of the cycle efficiency to pressure ratio.

In addition to the sensitivity analyses completed in this study, additional cycle dependencies should be examined. Particularly, the dependence of the cycle performance to cooler temperature, minimum temperature approach, and pressure drop should be explored. The latter is very important in the recuperated Brayton cycle and particularly so for the recompression cycle. The recuperated and recompression cycle efficiencies show a strong dependence on pressure ratio and would be expected to be very dependent on the cycle pressure drop.

The next phase of this work should examine the performance of the cycle for real heat sources. For this study, the hot source was able to transfer 100 MMBtu/hr to the working fluid regardless of the turbine inlet temperature. This may be a reasonable representation for the hot source in certain solar and nuclear energy applications, it is not an acceptable representation of fossil fuel heat sources which have an extremely wide temperature range. As was demonstrated, for recuperated Brayton cycles, cycle efficiency increases with turbine inlet temperature and recuperator effectiveness. However, increasing the turbine inlet temperature and the recuperator effectiveness will act to reduce the fraction of the available heat that can used in the cycle. These effects may mean that the recompression Brayton cycle needs to be incorporated into a combined cycle configuration.

As the analysis of the recompression CO_2 Brayton cycle focuses on more realistic and practical applications, systems studies should be performed to compare it to commercially available

alternatives such as subcritical and supercritical steam cycles. Because of the significantly lower technology readiness level of the recompression CO_2 cycle, estimates for appropriate operating conditions and estimates for loss terms will be more uncertain than for the very mature steam cycles. Hence, any system study comparing the implementation of these cycles should include sensitivity analyses on the key operating conditions and sources of losses.

The results of this study suggest that attempts to optimize the performance of the recompression CO_2 Brayton cycle need to factor in cost in the analysis. A number of sensitivity runs for this study showed that operating the cycle at peak efficiency may lead to very low values for specific power. It is recommended that the next phase of this work include additional cost surrogate variables. However, an optimum operating state cannot be reliably identified without a detailed design and accompanying engineering and materials selections allowing an accurate cost estimate.

1 Introduction

The Department of Energy (DOE) has recently shown an increased interest in the potential application of supercritical CO_2 (sCO_2) cycles for power generation. At the direction of the National Technology Laboratory (NETL), Energy Sector Planning and Analysis (ESPA) completed a literature review of prior studies and actual implementations of sCO_2 cycles entitled "Supercritical CO_2 Power Cycles Literature Survey". The literature review indicated that sCO_2 cycles appeared to offer some benefits compared to conventional power cycles, particularly with regard to possible reductions in size and cost but also in the opportunity for improved process efficiency. (1)

NETL funded exploratory work in the application of sCO_2 cycles in place of a supercritical Rankine cycle in an oxy-fired pressurized fluidized bed application. ESPA performed a review of that study and its accompanying Aspen Plus® model; the review supported the conclusion that the sCO_2 cycle could boost system efficiency by 3-4 percentage points. (2)

NETL further tasked ESPA to prepare a design basis for an internal system study that would answer some of the questions about the sCO_2 cycle that remained unanswered. These included the root cause of the cycle efficiency improvement, the role of the physical properties of the working fluid on the cycle performance, the sensitivity of the cycle performance to the operating conditions of the cycle, the role of the heat source in the applicability of the sCO_2 cycle, and a preliminary attempt to address whether the sCO_2 cycle was cost effective using surrogate cost variables.

In the course of developing this design basis, a detailed and extensive Brayton cycle analysis was performed to better understand at a fundamental level the dependence of the Brayton cycle performance on operating conditions, working fluid, supercritical fluid properties, and some cycle non-idealities. This white paper documents the results of that Brayton cycle analysis.

The focus of this study is on cycle performance, particularly efficiency. No cost estimates were performed. However, as a single indirect measure of cycle cost, some sensitivity analyses on specific power (net output divided by working fluid mass flow rate) were included.

The white paper first presents the results of the analysis of a basic closed Brayton cycle as a baseline. Some of the sensitivity runs suggested that non-idealities in CO_2 physical properties were influencing cycle performance. Therefore, an examination of the CO_2 physical properties as estimated by the Peng-Robinson equation of state with Boston-Mathias corrections (PR-BM), the National Institute of Standards equation of state (REFPROP), and the ideal gas equation of state were performed and the results compared. Next the analysis turned to recuperated Brayton cycles. This was further extended to two-stage recuperated Brayton cycles, frequently referred to as recompression Brayton cycles. Finally, the analysis was extended to recompression cycles with reheat.

2 Non-recuperated Brayton Cycle

The initial analysis of the Brayton cycle was performed on the simple cycle shown in Exhibit 2-1. Point A on the diagram represents the compressor in which work is performed (W_C) on the CO_2 to increase its pressure and temperature. At point B, the heat source transfers a fixed heat rate (Q_H) to the CO_2. It is assumed that the flow rate of CO_2 can be adjusted such that the temperature of the CO_2 entering the turbine at point C attains some specified turbine inlet temperature (TIT). The expansion of the CO_2 in the turbine produces work (W_E) and lowers the CO_2 temperature. Even in an ideal cycle, it is not possible for the expanded gas to return to the starting point temperature. Additional cooling (Q_C) is required at point D to close the cycle.

The equations for net power and efficiency are given in Exhibit 2-1. For any given heat input, Q_H, the efficiency increases as W_E increases, W_C decreases, and Q_C decreases.

In the initial cycle analyses, the cycle was assumed to operate ideally with ideal gas behavior and no energy losses. Non-idealities were introduced into the analysis one by one to examine their impact on the cycle performance individually.

Exhibit 2-1 Simple Brayton cycle without recuperation

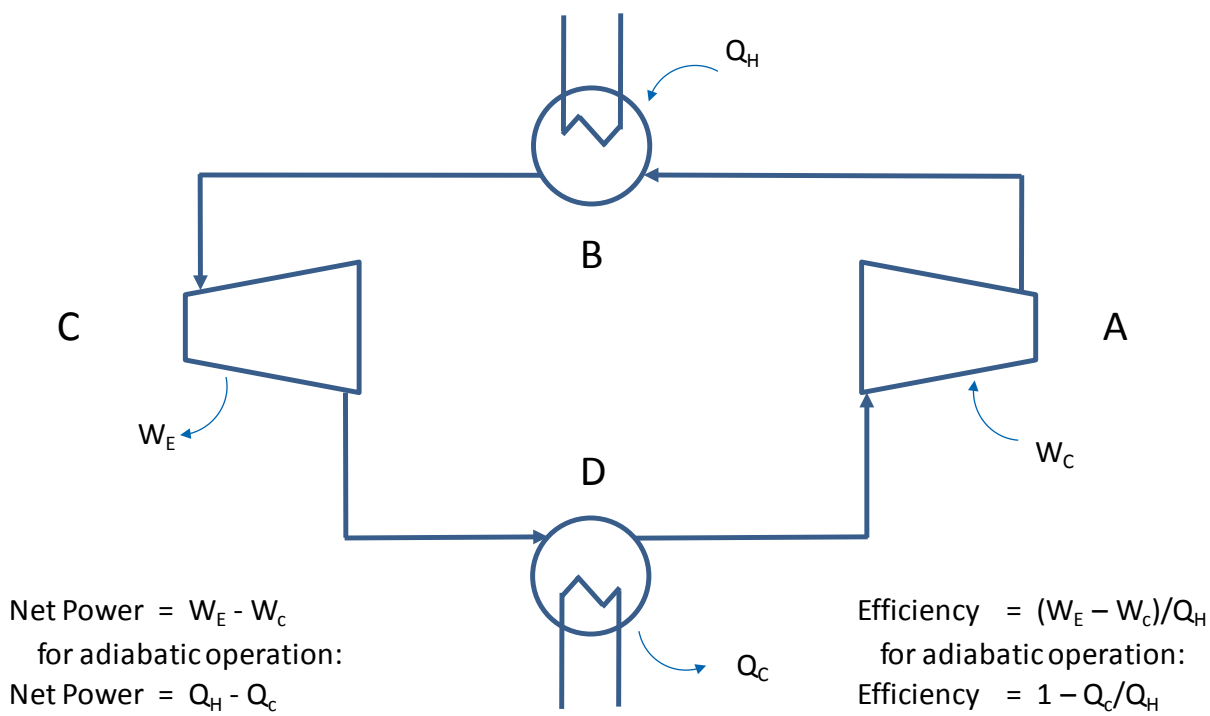

The cycle was analyzed for a fixed heat source of 100 MMBtu/hr with no heat losses other than the heat loss in the condenser. No losses were taken for auxiliary power, generator, or pressure drops in the cycle. Sensitivity analyses were performed to determine the cycle performance as a function of pressure ratio. Other cycle parameters were then varied to examine their impact on the cycle performance.

For an ideal closed non-recuperated cycle with ideal turbo-machinery (isentropic efficiencies of 1) the cycle efficiency does not depend on TIT (other than a slight effect due to the non-idealities of CO_2) but it does depend on pressure ratio (PR). For this cycle, the efficiency increases as PR increases. It starts off at zero for a pressure ratio of 1 and increases monotonically with PR. The maximum feasible pressure ratio occurs when the compressor exit temperature equals the turbine inlet temperature. If the TIT is high enough, the cycle efficiency approaches 1 when the pressure ratio approaches infinity. This is basically a restatement of the Carnot efficiency for this ideal cycle.

If the gas is ideal, the efficiency can be shown to be given by the following equation:

$$\eta = 1 - \left(\frac{1}{PR}\right)^{\frac{\gamma-1}{\gamma}} \qquad [1]$$

where η is the efficiency and γ is the ratio c_p/c_v. c_p is the heat capacity at constant pressure and c_v is the heat capacity at constant volume. (3)

2.1 Aspen Plus® Simulations of Simple Non-recuperated Brayton Cycle

Exhibit 2-2 shows the cycle parameters used for the initial sensitivity analyses.

Exhibit 2-2 Parameters used in Aspen Plus® simulations

Parameter	Value
Turbine inlet temperature	1300 °F
Cooler exit temperature	95 °F
Turbine exit pressure	1150 psia
Compressor isentropic efficiency	1.0
Turbine isentropic efficiency	1.0

The turbine inlet temperature and turbine exit pressure correspond to values used in a recently proposed application of supercritical CO_2 cycles for a conceptual power plant with an oxy-fired pressurized fluidized bed combustor (PFBC) heat source. The cooler exit temperature is just above the critical temperature for CO_2 (31 °C, 88 °F).

Exhibit 2-3 shows a plot of cycle efficiency versus PR for an ideal simple sCO_2 Brayton cycle.

Exhibit 2-3 Efficiency versus pressure ratio for a simple Brayton cycle with sCO_2 and 1300 °F TIT

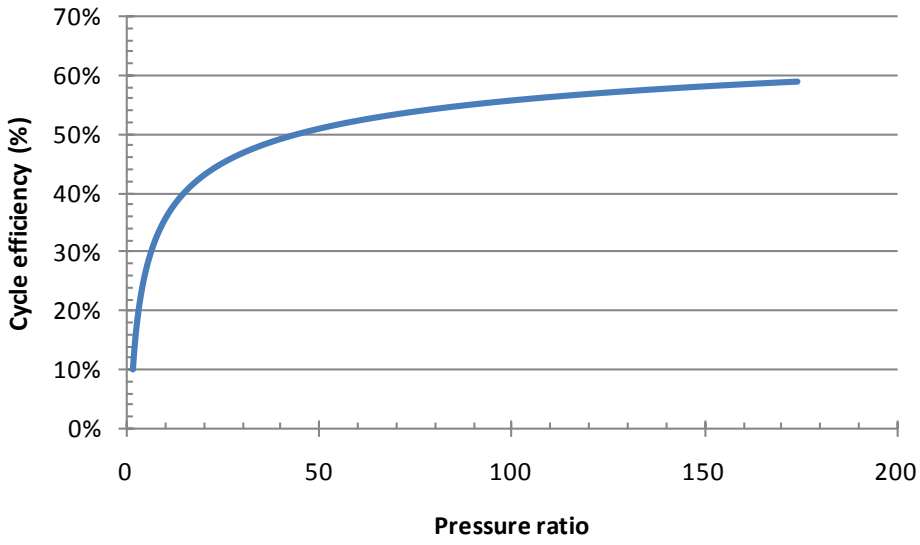

Exhibit 2-4 shows the same plot with another cycle efficiency curve with a TIT of 1800 °F demonstrating that the efficiency does not depend on TIT. Exhibit 2-5 shows the efficiency plot from Exhibit 2-3 overlaid with the results using Equation [1].

Exhibit 2-4 Impact of TIT on efficiency versus pressure ratio for a simple Brayton cycle with sCO_2

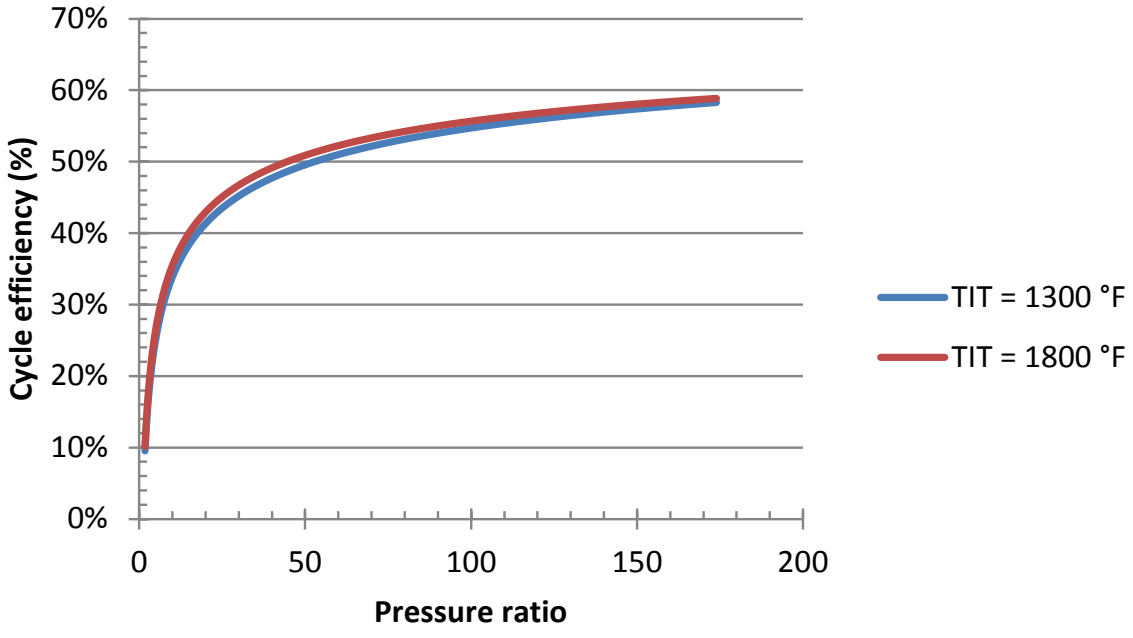

Exhibit 2-5 Efficiency versus pressure ratio for a simple Brayton cycle with sCO_2 and 1300 °F TIT

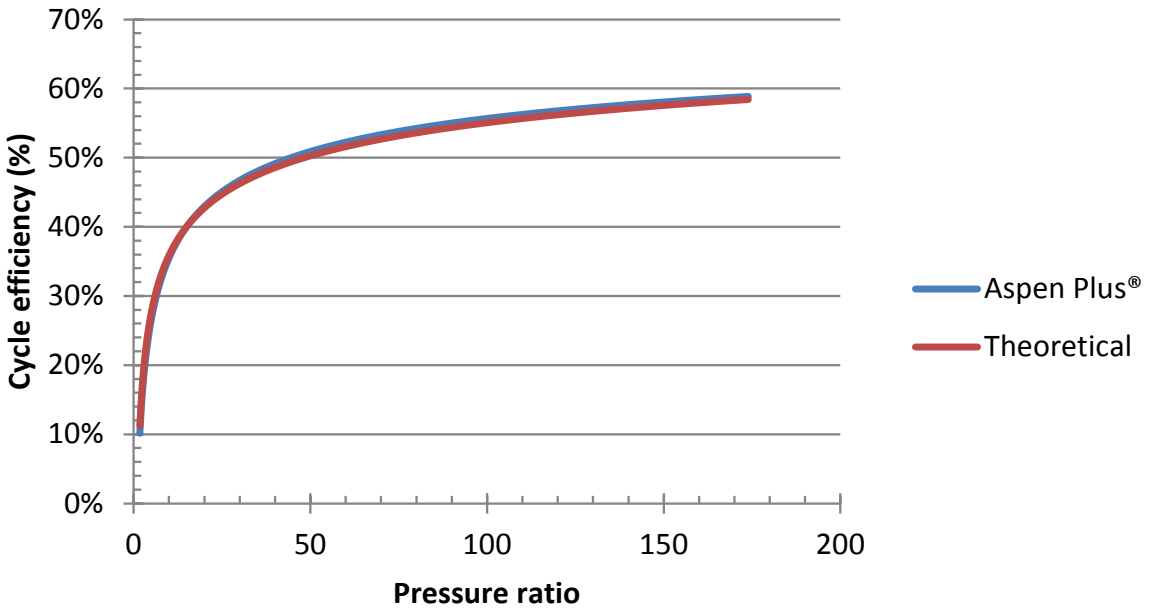

The simulation results are consistent with Equation [1] and show that for an ideal simple Brayton cycle, the efficiency increases monotonically with pressure ratio and is independent of TIT. Although operating at high pressure ratios may seem advantageous, beyond a pressure ratio of about 40, the curve flattens out so much that efficiency gains with increased pressure ratio are too small to be economical. This can be seen better by examining the specific power, i.e., the net cycle output divided by the working fluid mass flow rate. The specific power provides an indirect measure of relative cost, since, if all other factors are equal, a cycle with a smaller specific power than another cycle will require a proportionally greater working fluid flow to get the same net output, resulting in a greater cost.

Exhibit 2-6 shows a plot of specific power versus pressure ratio for an ideal Brayton cycle with a TIT of 1300 °F. The plot shows a maximum in the specific power at a pressure ratio just under 31. The existence of the maximum is both interesting and general. At PR = 1, the specific power is zero. As the pressure ratio increases, the specific power increases, but at an ever slowing rate until the rate becomes zero, then negative. If the pressure ratio increases further, at some point the power needed to compress the gas equals the power output from the turbine and the specific work again falls to zero.

Exhibit 2-6 Specific power versus pressure ratio for a simple Brayton cycle with sCO_2 and 1300 °F TIT

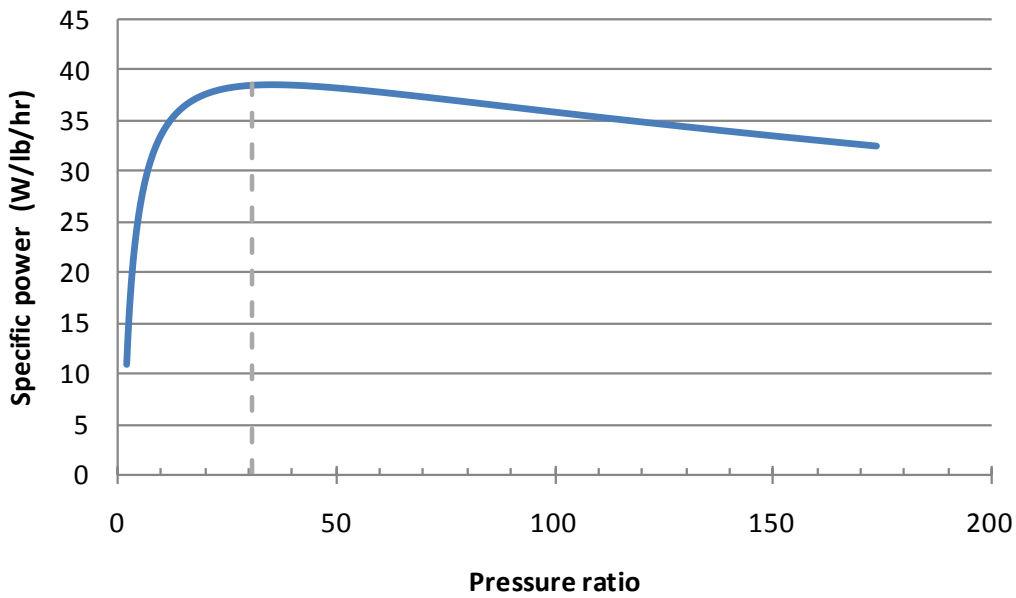

For an ideal simple Brayton cycle, that upper limit is given by:

$$\mathrm{PR} = \left(\frac{TIT}{T_a}\right)^{\left(\frac{\gamma-1}{\gamma}\right)} \qquad [2]$$

where Ta is the compressor inlet temperature and the temperatures are expressed in degrees absolute. (3)

Exhibit 2-7 shows the same plot as in Exhibit 2-6, but adds the specific power plot for an ideal Brayton cycle with a TIT of 1800 °F. It can be readily seen that the specific power has a strong dependence on TIT.

Exhibit 2-7 Specific power versus pressure ratio for a simple Brayton cycle with sCO_2 and 1300 °F and 1800 °F TIT

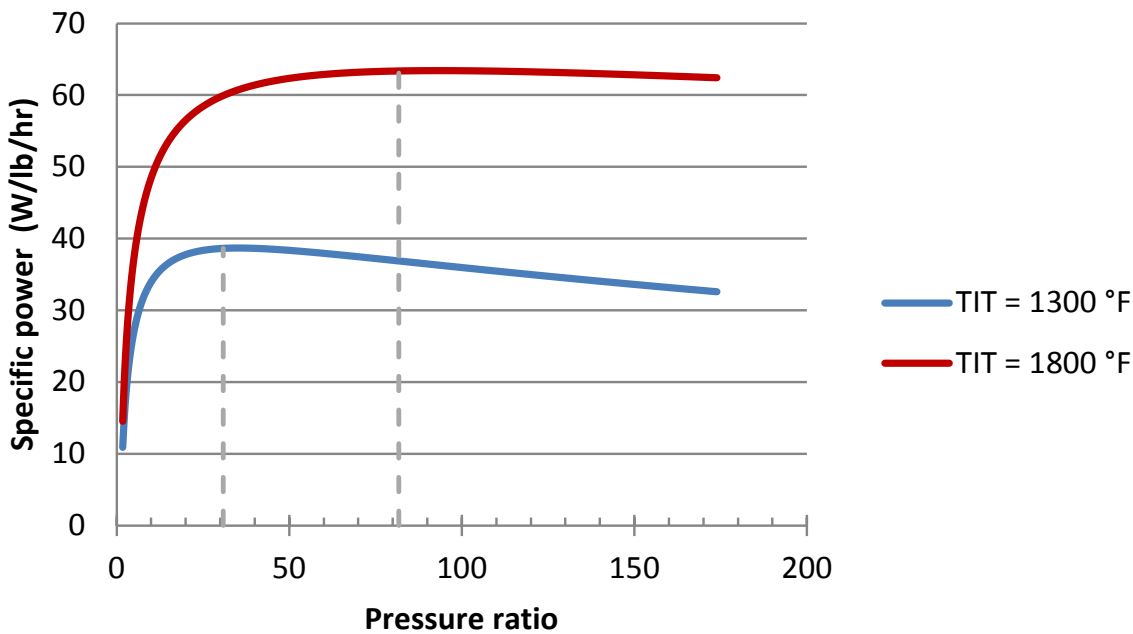

For an ideal Brayton cycle in which the working fluid heat capacity is constant, the specific power is given by the following equation:

$$\frac{w}{c_p T_a} = \left(\frac{TIT}{T_a}\right)\left(1 - \frac{1}{PR^{\left(\frac{\gamma-1}{\gamma}\right)}}\right) - \left(PR^{\left(\frac{\gamma-1}{\gamma}\right)} - 1\right) \qquad [3]$$

where w is the specific power. (3) This equation clearly shows the strong dependence of specific power on TIT. If this equation is differentiated with respect to PR, it can be shown that the maximum in specific power occurs at a pressure ratio where the compressor outlet temperature equals the turbine outlet temperature. Exhibit 2-8 and Exhibit 2-9 demonstrate this for two ideal simple Brayton cycles with TIT of 1300 °F and 1800 °F, respectively.

Exhibit 2-8 Simple Brayton cycle with sCO_2 and 1300 °F TIT, turbine and compressor exit temperatures

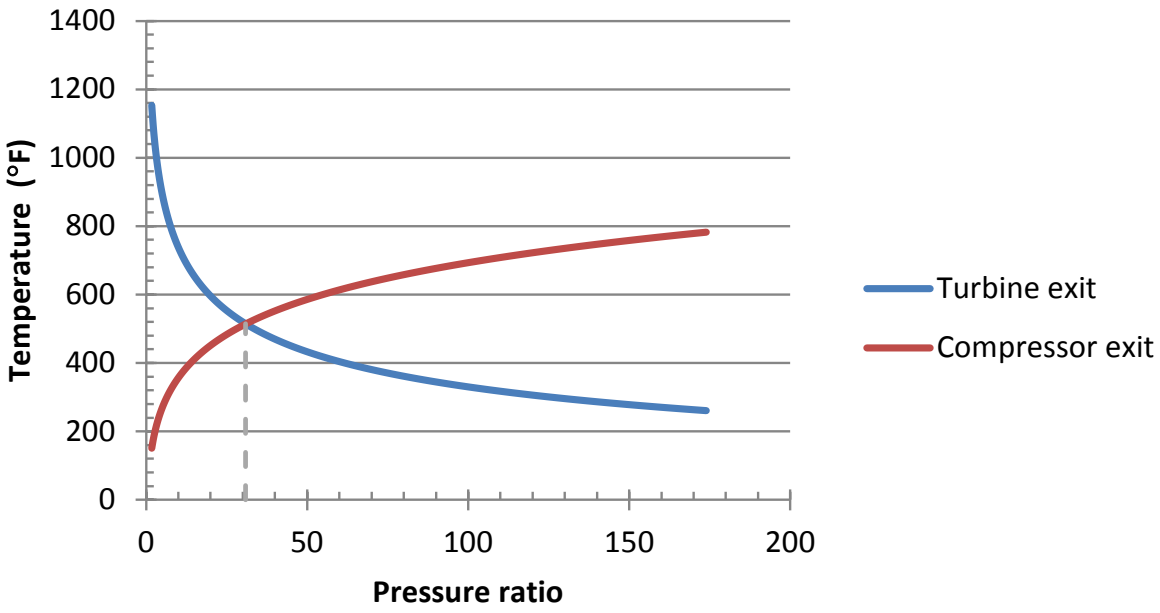

Again, these results are only valid for ideal simple Brayton cycles.

Exhibit 2-9 Simple Brayton cycle with sCO_2 and 1800 °F TIT, turbine and compressor exit temperatures

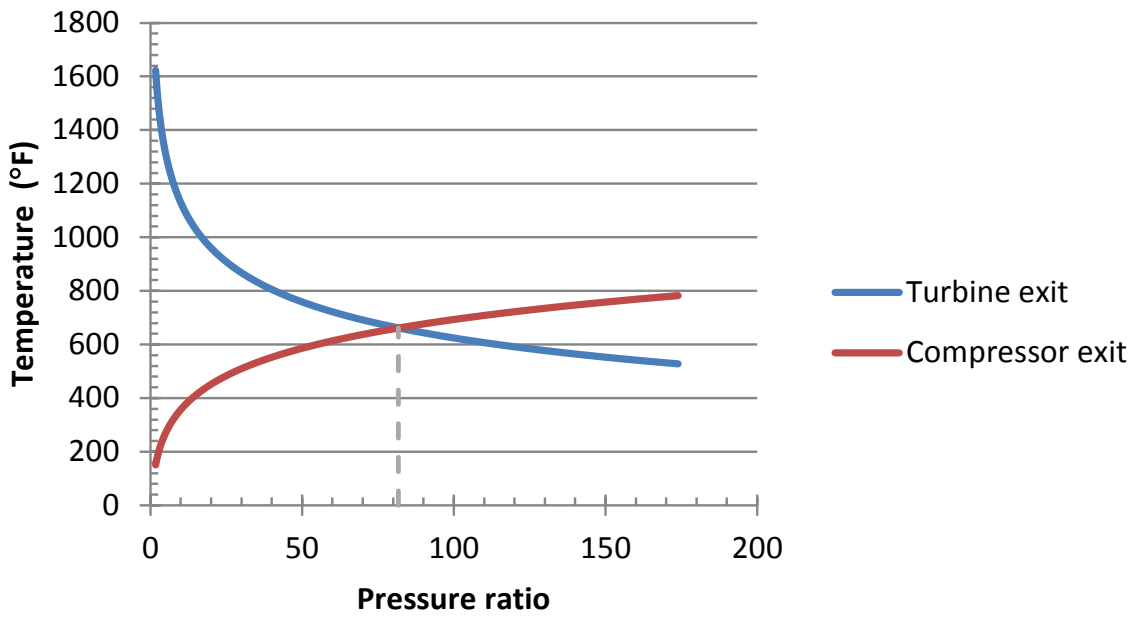

2.2 Impact of Working Fluid

In addition to sCO_2, the Brayton cycle simulations were run with other working fluids. Exhibit 2-10 shows a plot of cycle efficiency versus pressure ratio for three working fluids, argon (Ar), nitrogen (N_2), and CO_2. For each working fluid, two sensitivity runs were performed, one with the ideal gas equation of state, and one using the PR-BM equation of state. The cycle conditions are the same as those shown in Exhibit 2-2.

For any working fluid, the difference in the ideal run and the PR-BM run reflects the impact of fluid non-ideality on the cycle efficiency. This impact is greater for CO_2 than the other fluids and will be examined in more detail in Section 3.

The reason for the large difference in the cycle efficiencies for the three working fluids is the difference in the working fluid γ. The values of γ for CO_2, N_2, and Ar at the turbine entrance are 1.2, 1.34, and 1.67, respectively.

Exhibit 2-11 shows the specific power versus pressure ratio for the three working fluids. All runs were based on the PR-BM equation of state. Each working fluid showed a maximum in specific power. This maximum decreased in magnitude and occurred at smaller pressure ratios for the three species in the order CO_2, N_2, and Ar.

Exhibit 2-10 Cycle efficiency as a function of pressure ratio

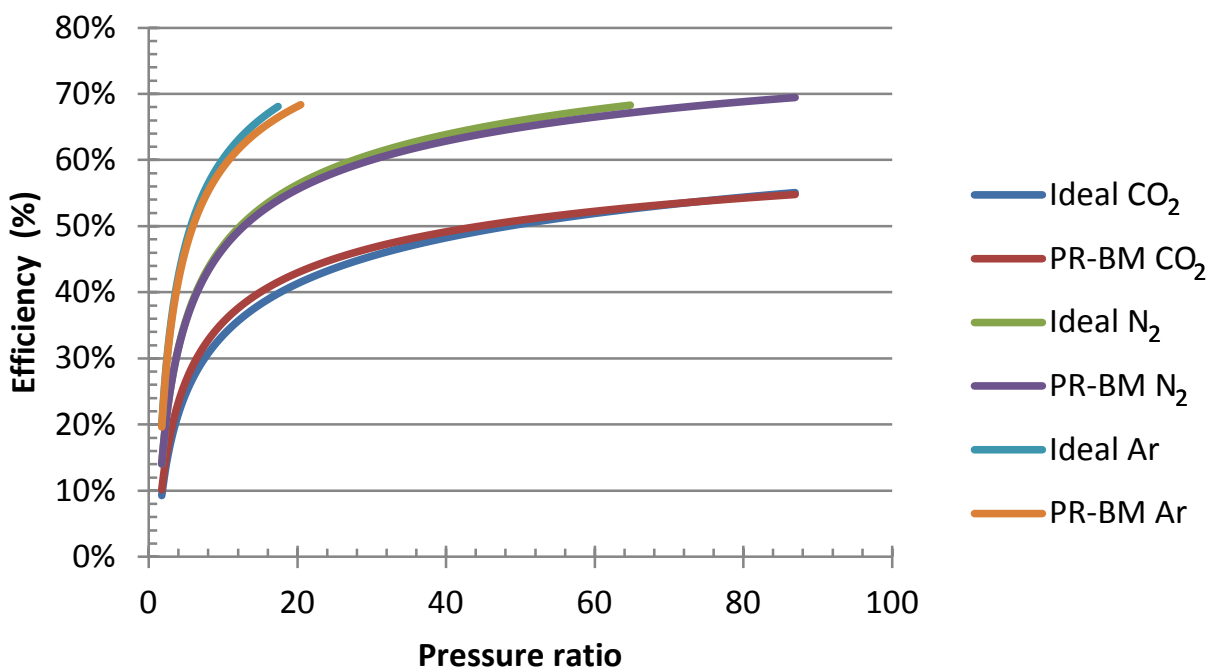

Exhibit 2-11 Specific power as a function of pressure ratio

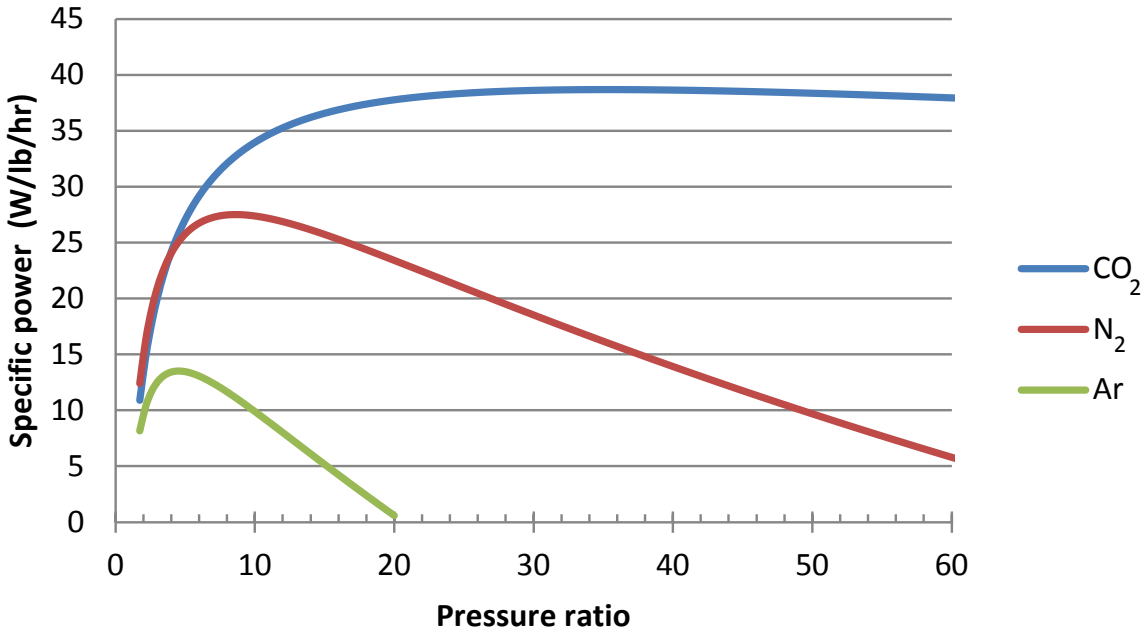

2.3 Impact of Turbine Inlet Temperature

The simulations performed at a turbine inlet temperature of 1300 °F were repeated at turbine inlet temperatures of 1500 °F and 1700 °F. These results are shown in Exhibit 2-12.

Exhibit 2-12 Cycle efficiency versus pressure ratio at different TIT

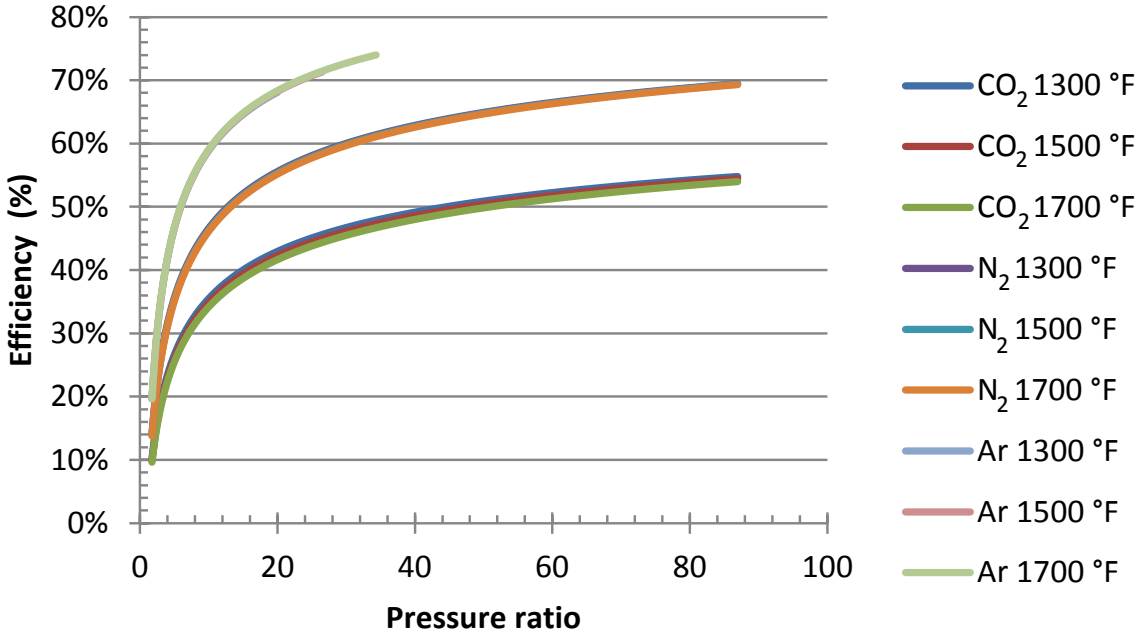

For each working fluid the results at the three settings for TIT overlay each other. This again confirms the conclusion that for an ideal Brayton cycle, the overall efficiency is independent of turbine inlet temperature. Any observed dependence on turbine inlet temperature is a result of non-idealities in the working fluid. This latter effect is shown in Exhibit 2-13. This exhibit plots cycle efficiency versus TIT for eight different pressure ratios using CO_2 as the working fluid. At low values of PR, the plots are horizontal. As the PR increases, the plots show a slight, ever increasing, inverse dependence on turbine inlet temperature.

The analogous plot for N_2 is shown in Exhibit 2-14. It can be seen that the same trend in dependency on turbine inlet temperature occurs but the effect is much less pronounced. The analogous data for Ar showed an imperceptible dependence on turbine inlet temperature.

Exhibit 2-13 CO_2 Brayton cycle efficiency versus turbine inlet temperature

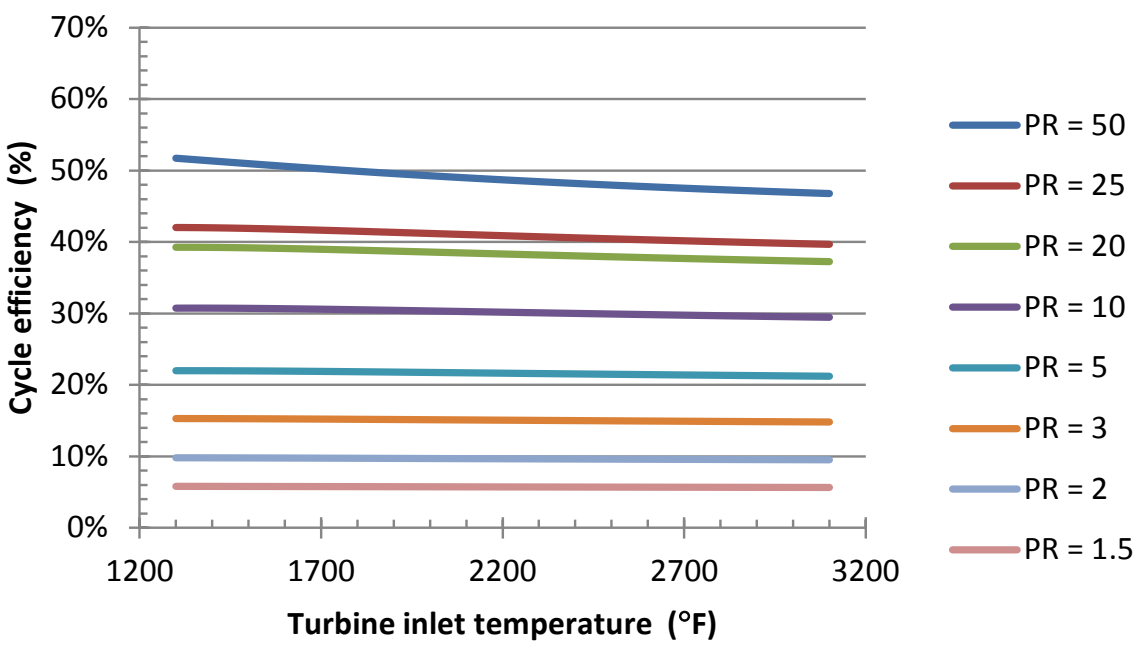

Exhibit 2-14 N_2 Brayton cycle efficiency versus turbine inlet temperature

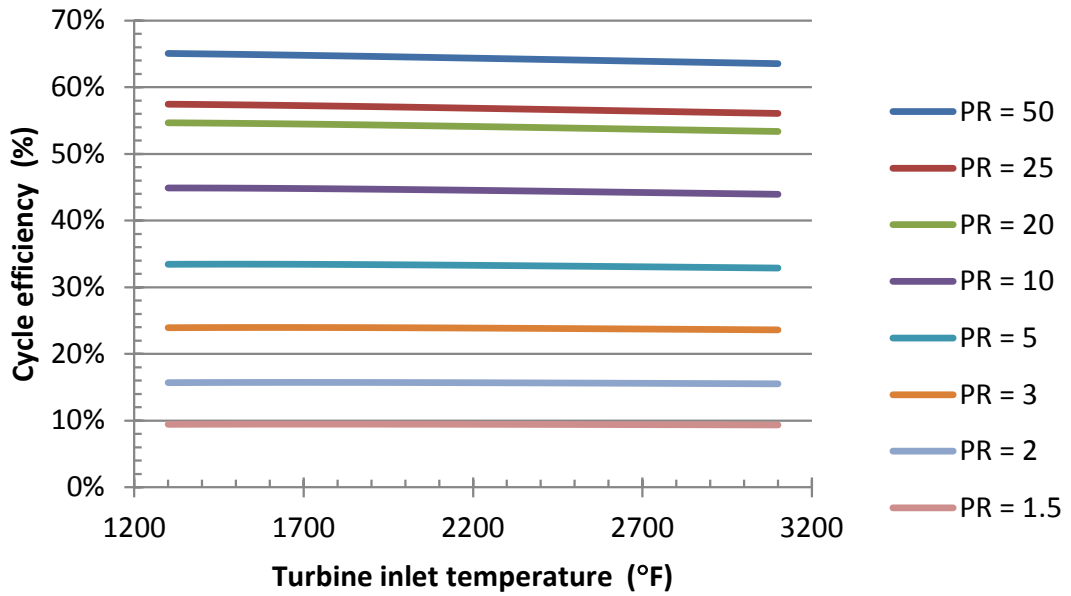

Exhibit 2-15 shows the dependence of specific power on turbine inlet temperature for the three working fluids. The specific power increases with turbine inlet temperature at any given pressure ratio for all three fluids. Similarly, the maximum specific power increases with turbine inlet temperature for each fluid, as does the pressure ratio at which the maximum occurs.

Exhibit 2-15 Brayton cycle-specific power dependence on turbine inlet temperature

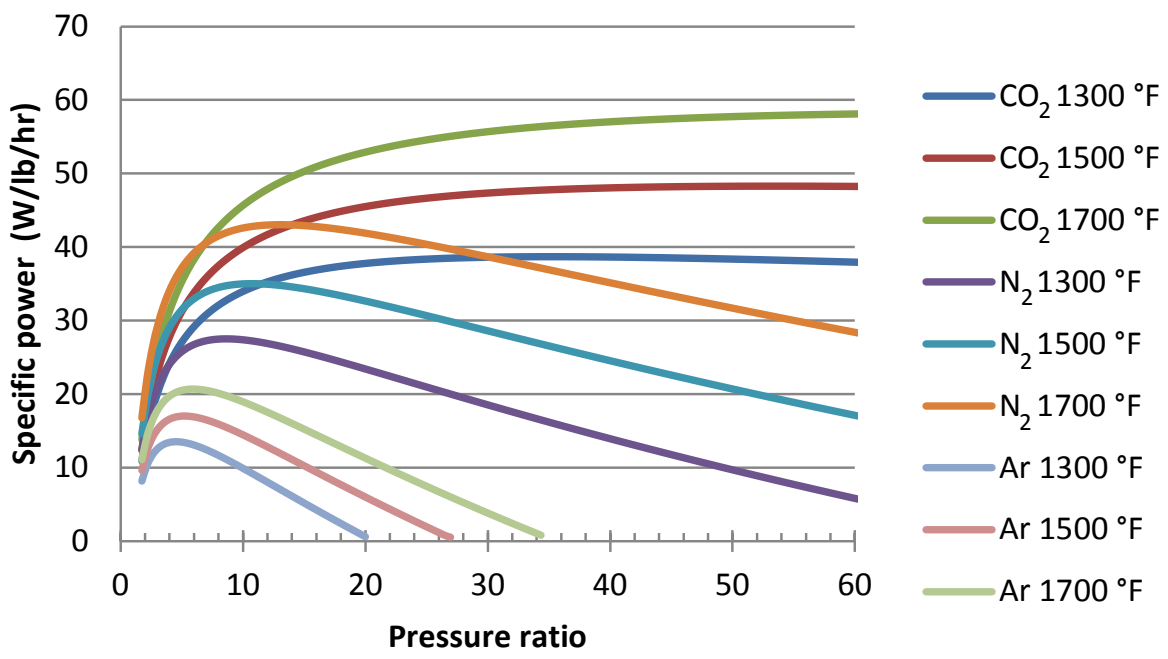

2.4 Impact of Turbine and Compressor Efficiency

The results presented to this point are only valid for ideal closed Brayton cycles for which the turbomachinery efficiencies are 1, and no other losses are taken. This section will examine the impact of compressor and turbine efficiencies less than 1 on the Brayton cycle performance. The cycle operating conditions will be the same as in Exhibit 2-2 unless explicitly noted.

Exhibit 2-16 shows the Brayton cycle efficiency versus pressure ratio for CO_2 at six different values for the turbine isentropic efficiency. For any turbine efficiency less than 1, the cycle efficiency versus pressure ratio shows a maximum efficiency and the pressure ratio at which the maximum efficiency occurs decreases as the turbine efficiency decreases.

Exhibit 2-17 shows an analogous plot for the specific power. As with the efficiency, the specific power decreases with decreasing turbine efficiency and the pressure ratio at the maximum specific power decreases as the pressure ratio decreases.

Exhibit 2-16 Brayton cycle efficiency dependence on turbine isentropic efficiency

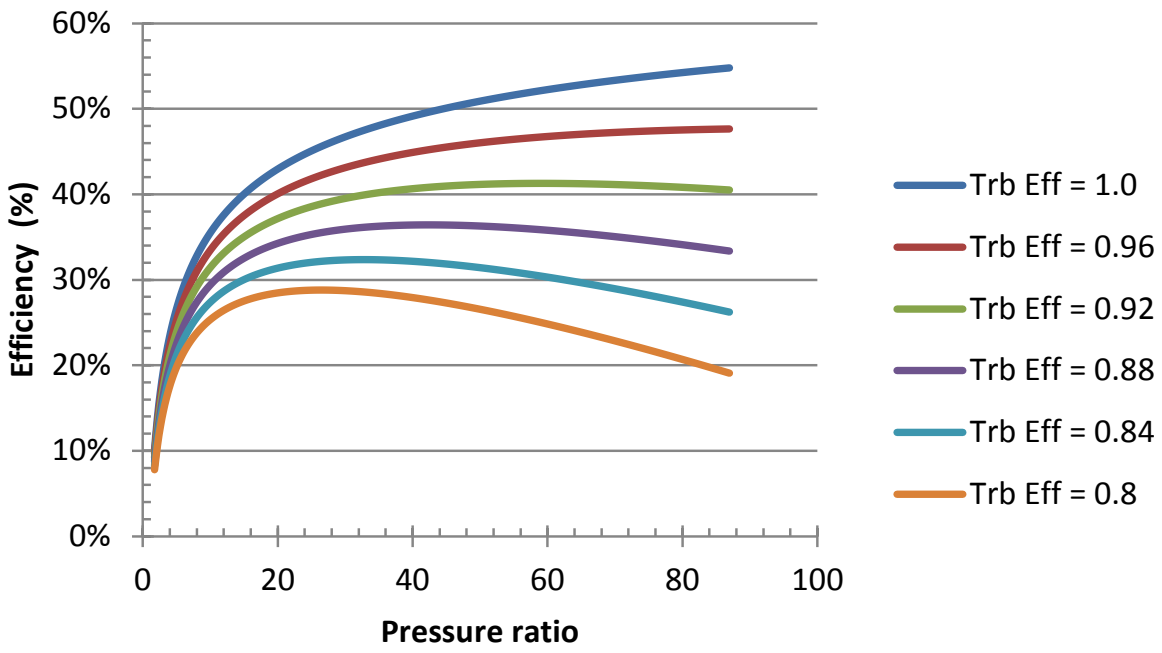

Exhibit 2-17 Brayton cycle-specific power dependence on turbine isentropic efficiency

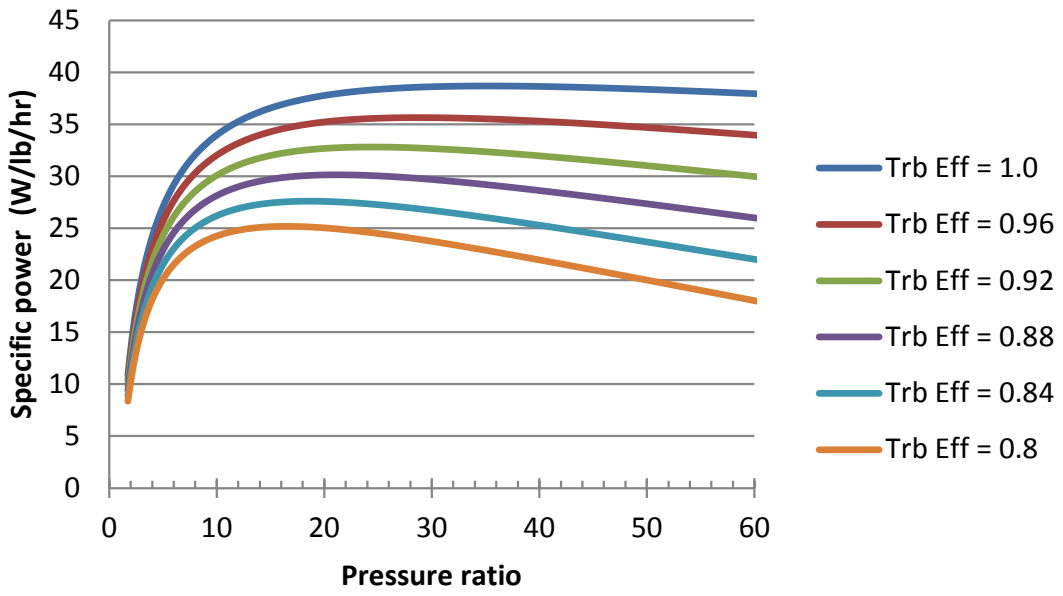

Exhibit 2-18 and Exhibit 2-19 are similar to Exhibit 2-16 and Exhibit 2-17, respectively, except that in these plots, the compressor efficiency is varied. As expected, the curves for variation in compressor efficiency show the same trends as the curves for variation in turbine efficiency. The major difference is that the impact of a drop in turbine efficiency is much more significant than a drop in compressor efficiency. At a pressure ratio of 20, a given drop in turbine efficiency results in a 3.6 times greater drop in cycle efficiency and a 2 times greater drop in specific power than for the same drop in compressor efficiency.

Exhibit 2-18 Brayton cycle efficiency dependence on compressor isentropic efficiency

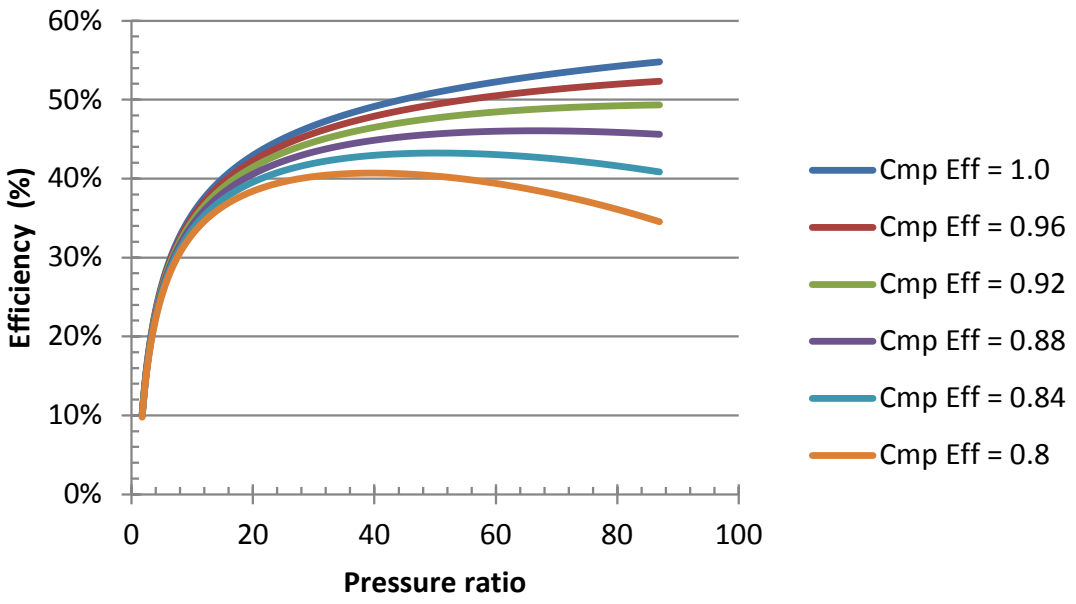

When the turbine efficiency drops, there is less output from the turbine and the turbine exit temperature increases. Both of these effects act to lower cycle efficiency. The lower turbine output lowers the net cycle output and the higher turbine exit temperature increase the Q_C duty. When the compressor efficiency decreases, more power is required for the compressor and the compressor exit temperature increases. In this case, the two effects have opposing influences on cycle efficiency. The increased compressor power lowers cycle efficiency by decreasing net cycle output. However, the increase in compressor exit temperature spares heat from the hot source allowing a greater working fluid flow and a higher net cycle output. Thus the increase in compressor exit temperature partially offsets the increase in compressor power.

Exhibit 2-19 Brayton cycle-specific power dependence on compressor isentropic efficiency

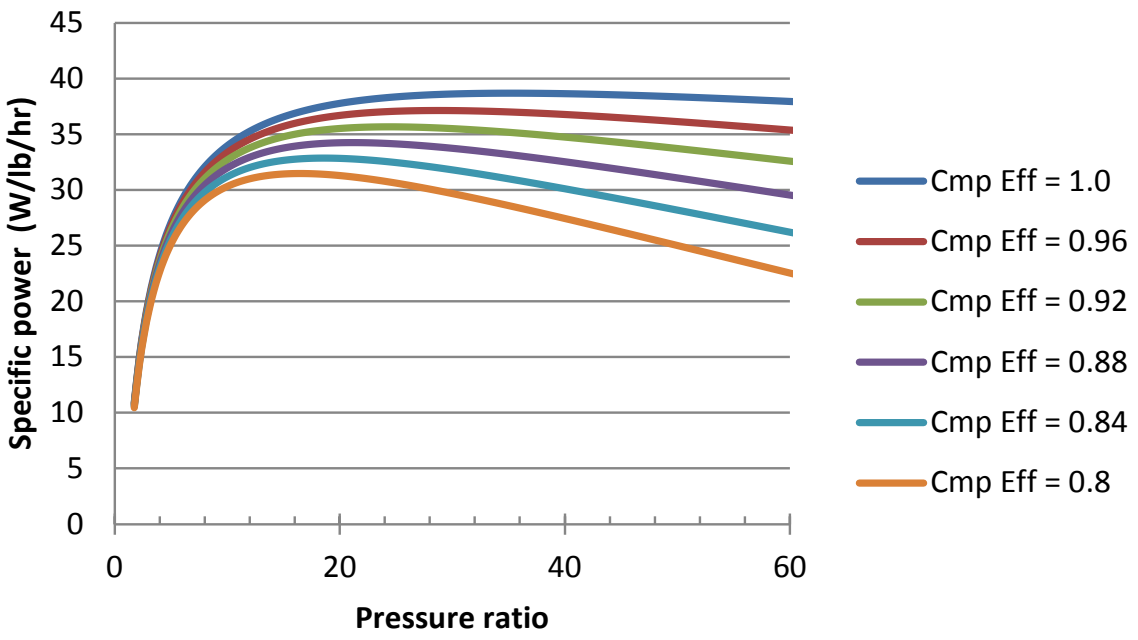

Exhibit 2-20 shows the impact on cycle efficiency when both the turbine and compressor isentropic efficiencies are lowered. Exhibit 2-21 shows the analogous impact on specific power. The drop in specific power from a simultaneous drop in turbine and compressor efficiency is cumulative and linear. On the other hand, a simultaneous drop in turbine and compressor efficiency has less impact on lowering cycle efficiency as the sum of the efficiency drops that would occur if the turbine and compressor efficiencies were lowered individually.

The most significant impact of lowering turbo-machinery efficiency is to lower both the cycle efficiency and specific power. Another impact of non-ideal turbo-machinery is that the cycle efficiency shows a maximum at some pressure ratio. The lower the turbo-machinery efficiency, the lower the maximum cycle efficiency will be and the lower the pressure ratio at which the maximum occurs will be.

Exhibit 2-20 Brayton cycle efficiency dependence on turbine and compressor isentropic efficiency

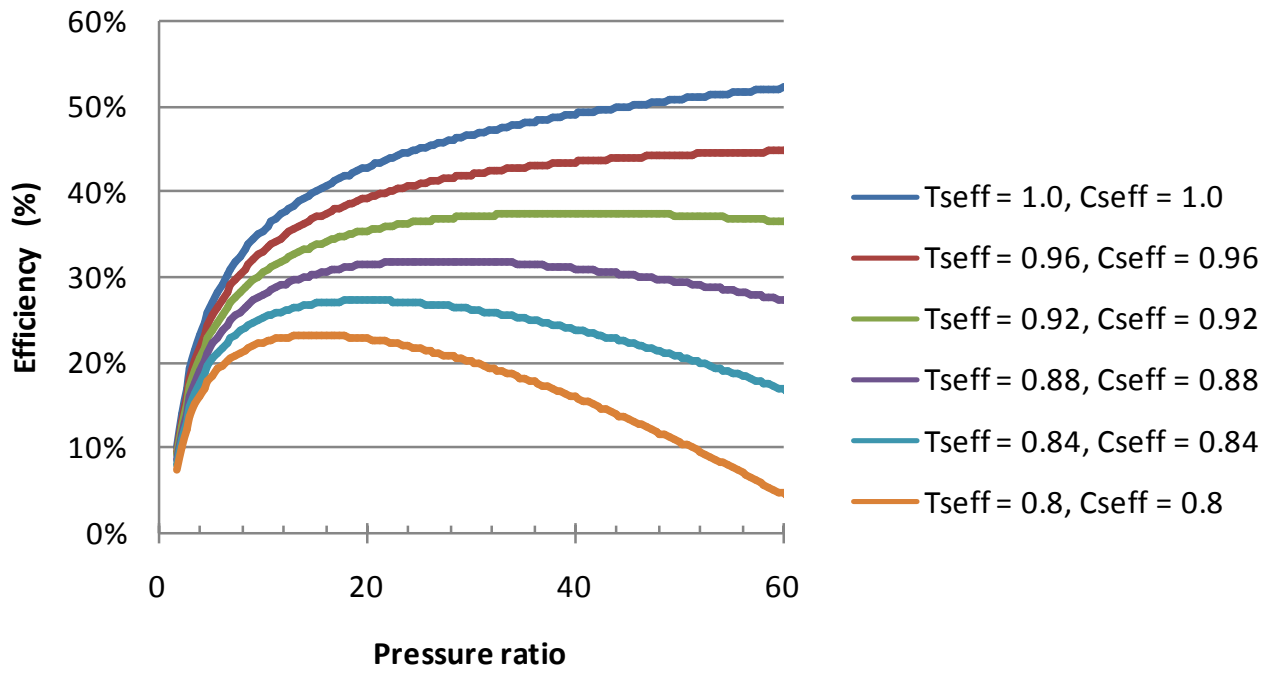

Exhibit 2-21 Brayton cycle-specific power dependence on turbine and compressor isentropic efficiency

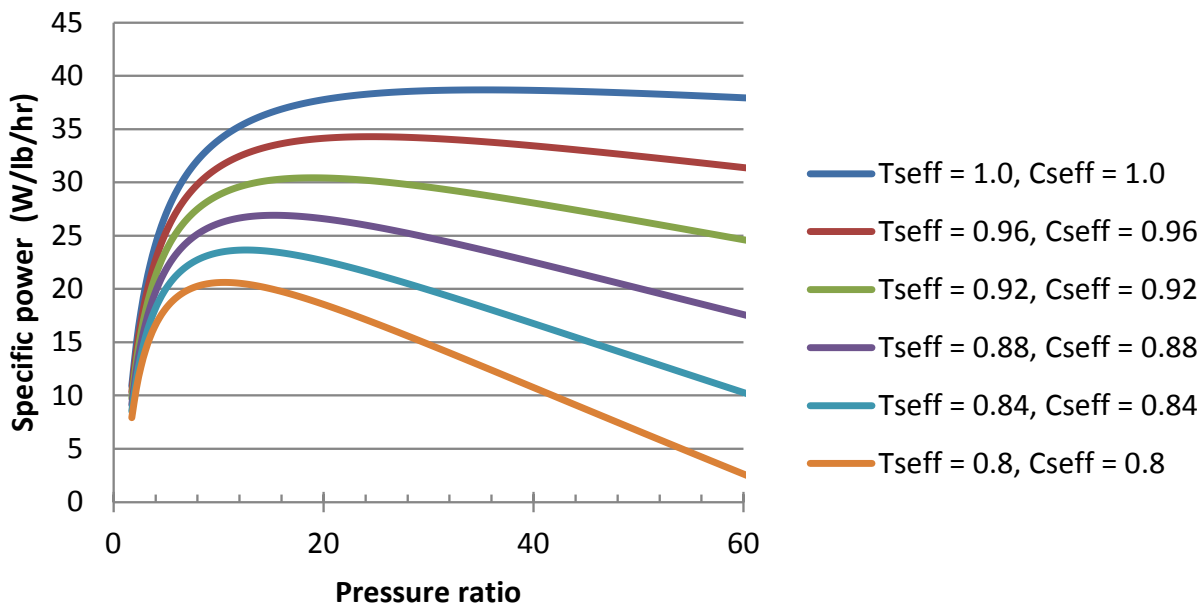

2.5 Impact of Turbine Exit Pressure

The final sensitivity performed for the simple non-recuperated Brayton cycle was to examine the impact of varying the turbine exit pressure. This sensitivity is only being reported for CO_2 as turbine exit pressure does not have a significant impact on the Brayton cycle performance for either N_2 or Ar.

Exhibit 2-22 shows the cycle parameters used for this sensitivity analysis.

Exhibit 2-22 Parameters used in Aspen Plus® simulations

Parameter	Value
Turbine inlet temperature	1300 °F
Cooler exit temperature	95 °F
Compressor isentropic efficiency	0.85
Turbine isentropic efficiency	0.927

Exhibit 2-23 shows the impact of turbine exit pressure on the cycle efficiency. This figure shows plots of cycle efficiency versus pressure ratio at 11 different values for the turbine exit pressure. Starting with a turbine exit pressure of 100 psia, as the turbine exit pressure increases, the cycle efficiency starts to increase until the turbine exit pressure reaches approximately 1200 psia. As the turbine exit pressure increases further beyond 1200 psia, the cycle efficiency falls until the turbine exit pressure reaches 3000 psia. Beyond this point, the cycle efficiency becomes less and less sensitive to the turbine exit pressure.

Exhibit 2-24 is a plot of the Brayton cycle maximum efficiency versus turbine exit pressure. As noted previously, the peak in cycle efficiency occurs at a turbine exit pressure of approximately 1200 psia. This occurs at a pressure ratio of approximately 33. The results suggest that the maximum cycle efficiency occurs when the minimum CO_2 pressure in the cycle is slightly above the critical pressure (7.39 MPa, 1070 psia).

Note the large rate of decrease in maximum cycle efficiency in the region of the maximum. The maximum cycle efficiency drops almost two percentage points with a 100 psia drop in the turbine exit pressure.

The results suggest that the properties of CO_2 in the supercritical fluid state are acting to increase cycle efficiency. This will be investigated further in the following section.

Exhibit 2-23 Brayton cycle efficiency dependence on turbine exit pressure (psia)

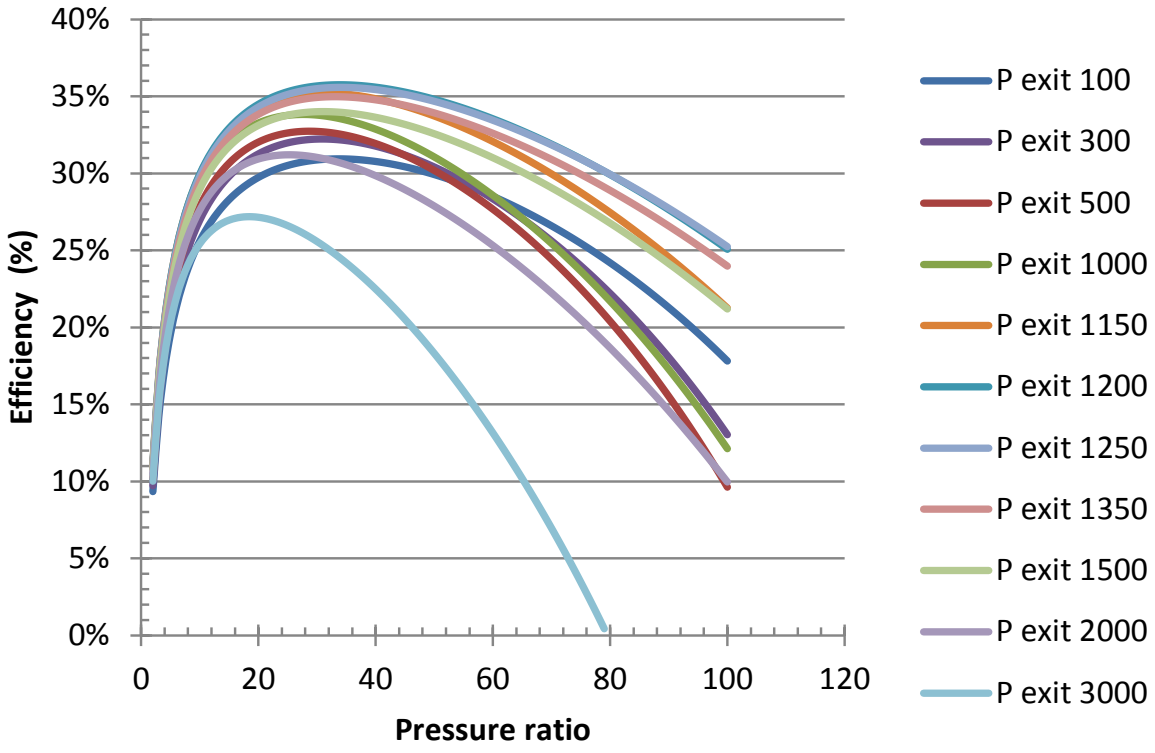

Exhibit 2-24 Maximum Brayton cycle efficiency dependence on turbine exit pressure

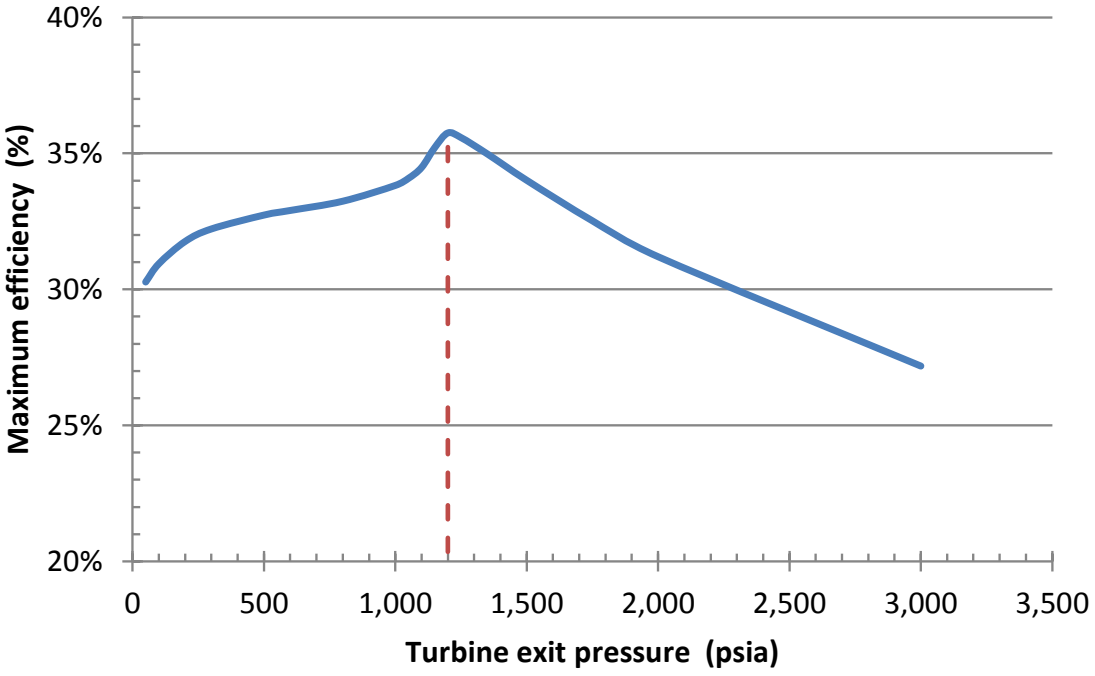

3 CO_2 Physical Properties

The results from the previous section suggest that changes in the physical properties of carbon dioxide near the critical point are contributing to increases in efficiency for a Brayton cycle based on CO_2. To investigate this further, a series of sensitivity runs was performed in Aspen Plus® on CO_2 using different physical property models. The sensitivity runs focus on the vicinity around the critical point.

Exhibit 3-1 shows a series of plots of CO_2 density versus temperature at eight different pressures (psia) using the PR-BM equation of state. The density increases markedly as the CO_2 passes the critical point and enters the supercritical fluid state.

Exhibit 3-1 CO_2 density versus temperature, pressure (psia)

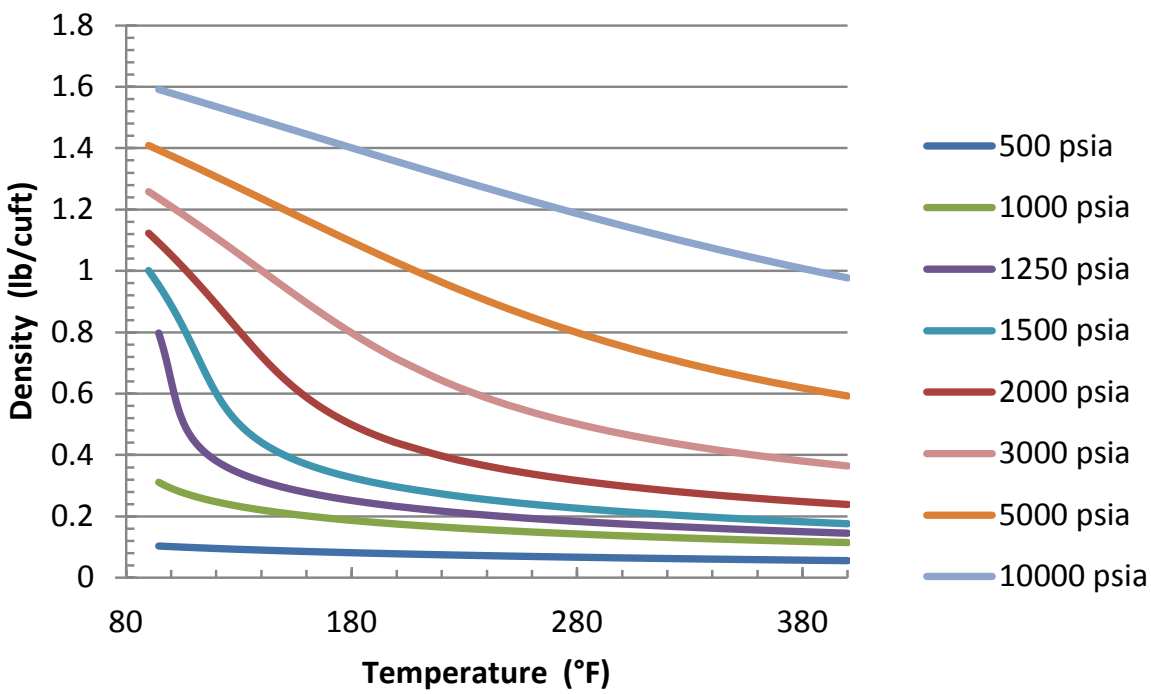

Exhibit 3-2 shows an analogous plot of the CO_2 heat capacity, c_p. In this case there is a near singularity in the plot at the critical point. Exhibit 3-3 shows the dependence of γ (c_p/c_v) for CO_2 on pressure and temperature. For an ideal gas, c_p, c_v, and c_p/c_v are all independent of pressure. For a simple CO_2 Brayton cycle operating at its peak efficiency, the CO_2 entering the compressor will be just above the critical point. The supercritical fluid CO_2 properties in this region reduce the work of compression needed and boost cycle efficiency. The large changes in physical property values occurring in this region for CO_2 point to the need for an accurate equation of state. The accuracy of the PR-BM equation of state was tested by comparing it to results obtained using REFPROP.

Exhibit 3-2 CO_2 c_p versus temperature, pressure (psia)

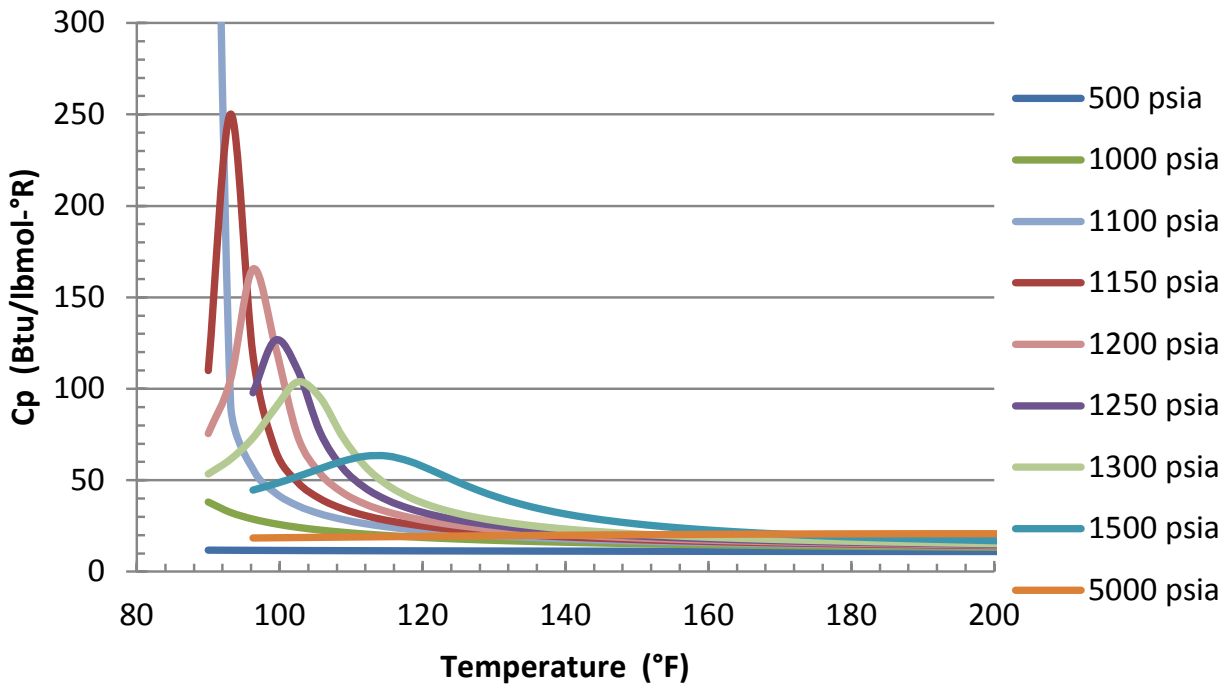

Exhibit 3-3 CO_2 c_p/c_v versus temperature, pressure (psia)

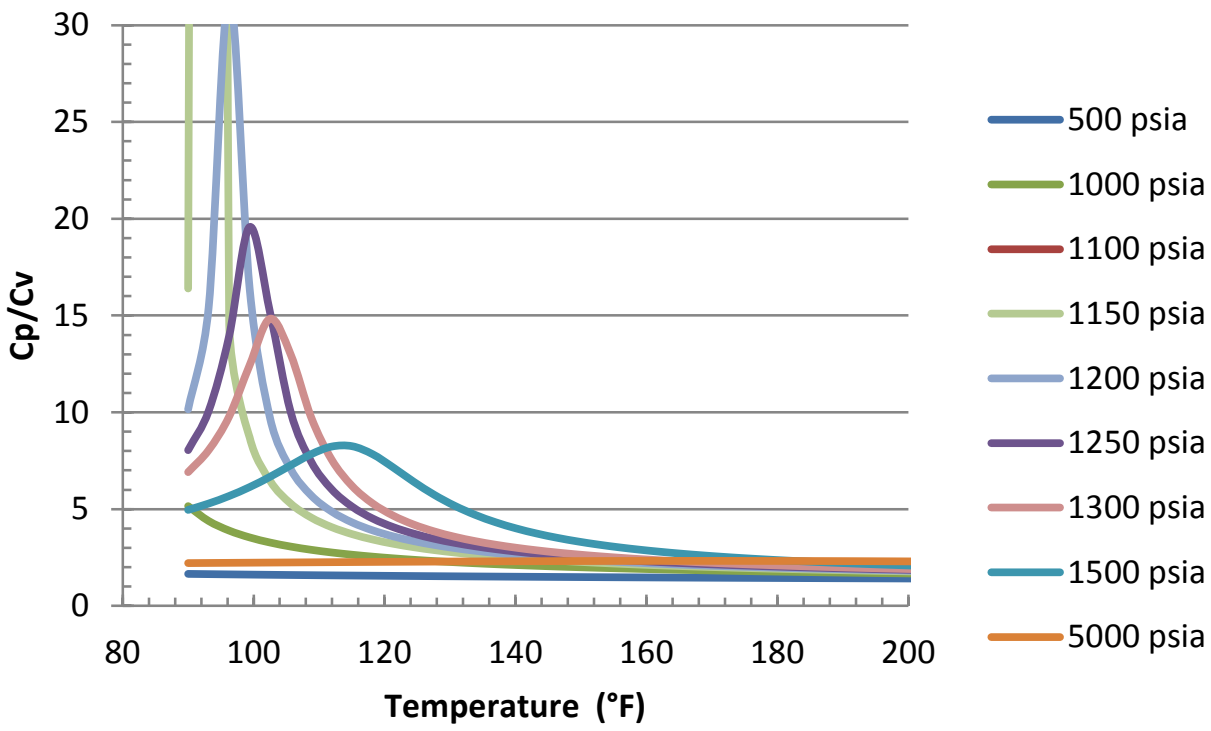

Exhibit 3-4, Exhibit 3-5, and Exhibit 3-6 show the same physical property dependencies for CO_2 as shown in Exhibit 3-1, Exhibit 3-2, and Exhibit 3-3, respectively, except the values were calculated using REFPROP.

Exhibit 3-4 CO_2 density versus temperature, pressure (psia)

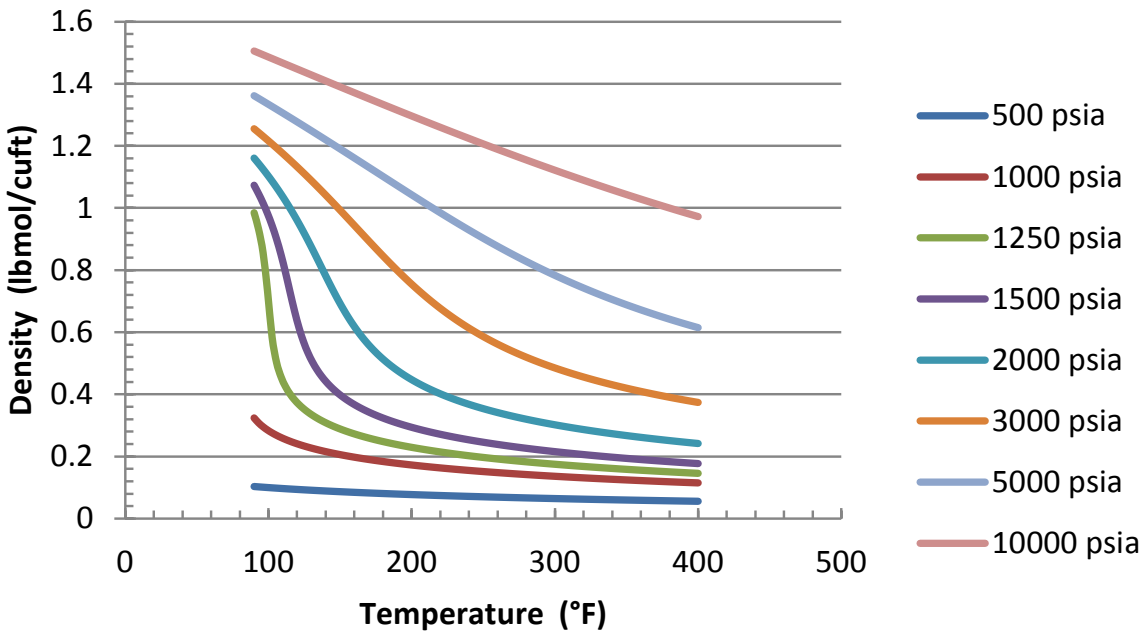

The differences in the property values calculated using PR-BM and REFPROP were significant for only a small region near the critical point. There was no significant difference in the estimated cycle efficiency using the two physical property methods. Because of its relative simplicity, the PR-BM equation of state was used for the remainder of the analysis in this study.

Exhibit 3-5 CO_2 c_p versus temperature, pressure (psia)

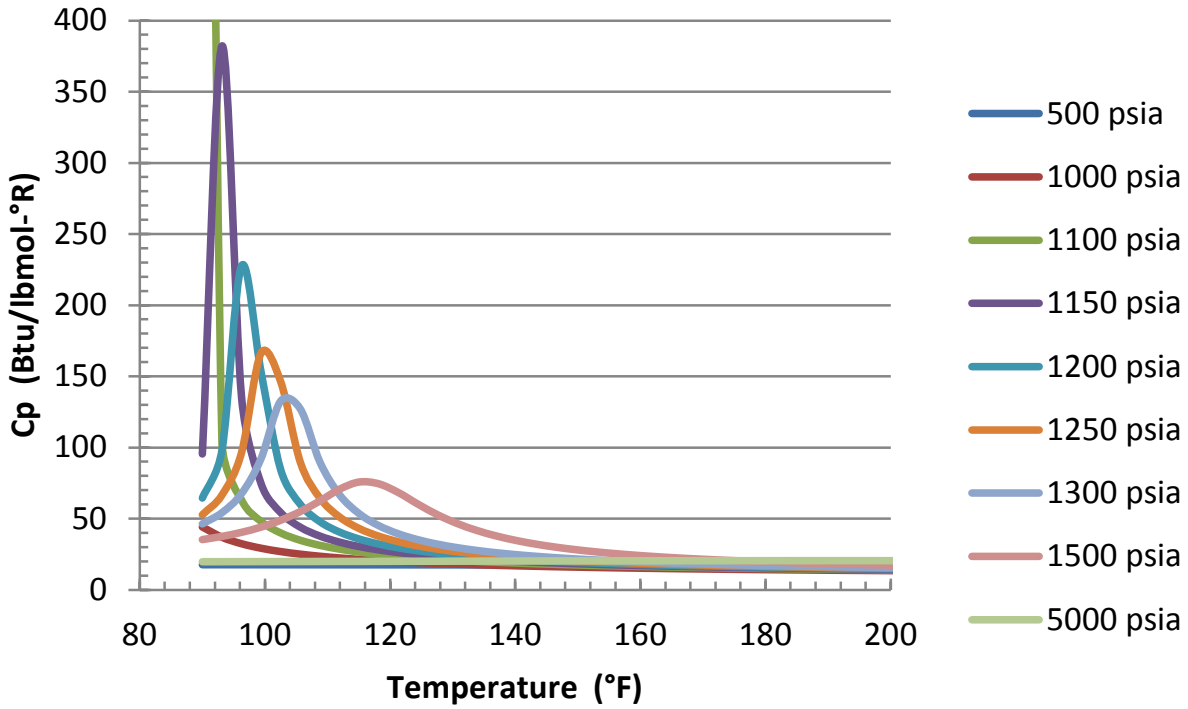

Exhibit 3-6 CO_2 c_p/c_v versus temperature, pressure (psia)

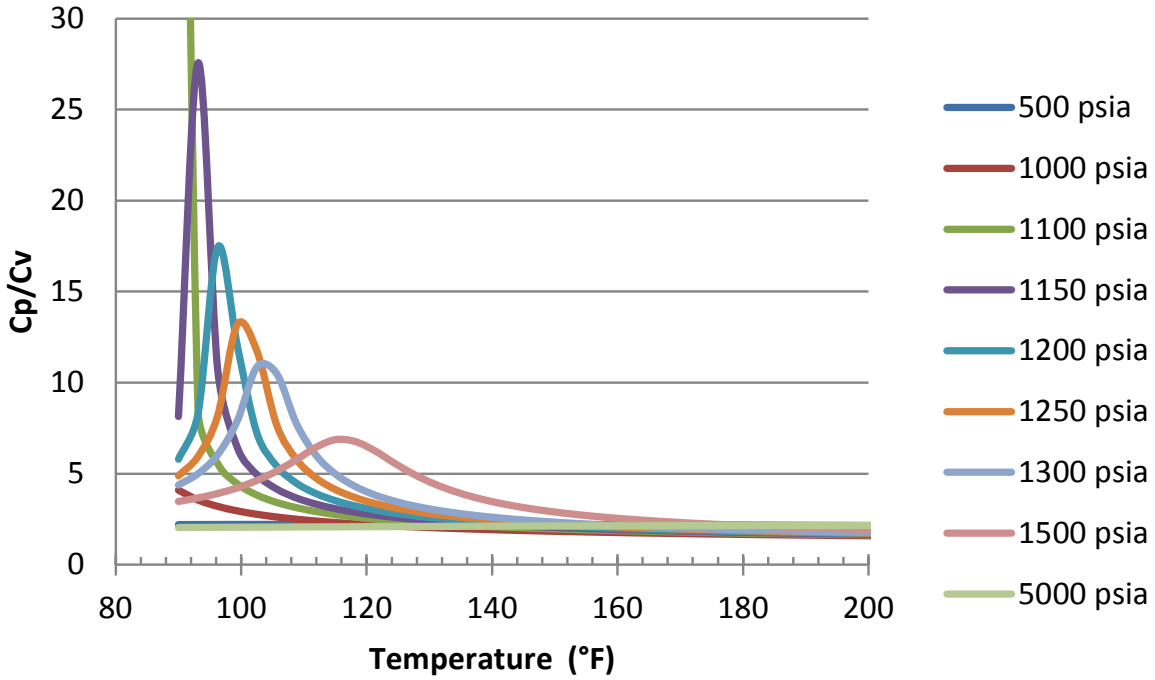

4 Recuperated Brayton Cycle

Exhibit 4-1 shows a block flow diagram (BFD) for a slightly more complex variant of the Brayton cycle.

Exhibit 4-1 Simple Brayton cycle with recuperation

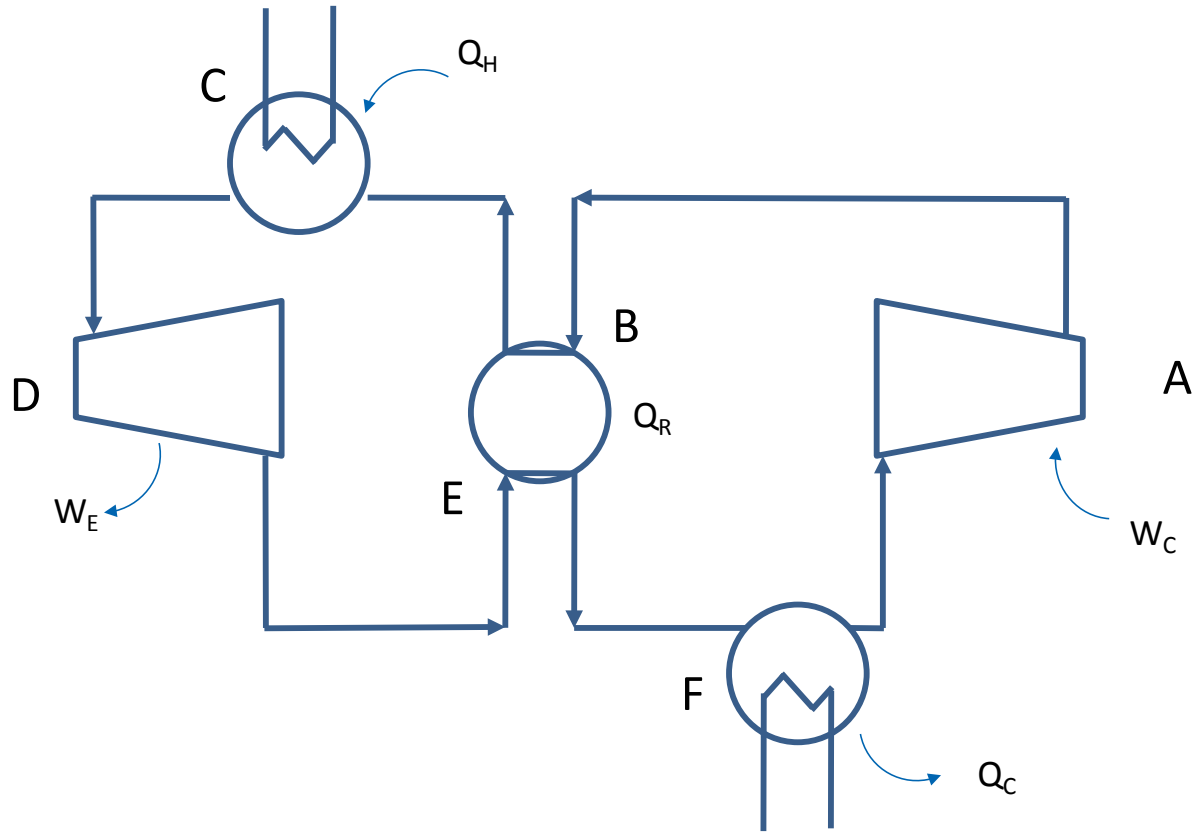

The cycle has the same elements as the previously analyzed cycle except that a recuperator has been added. The recuperator exchanges heat between the expanded CO_2 effluent from the turbine and the compressed CO_2 exiting the compressor. Obviously, the recuperated cycle can only work if the temperature of the turbine exhaust exceeds the temperature of the compressor exhaust. The total amount of heat transferred in the recuperator is Q_R. Recuperation raises the inlet temperature to the heat source allowing more CO_2 to pass through the cycle and increasing cycle output. However, as the amount of recuperation increases, the cycle pressure ratio must fall, which acts to decrease cycle output. Clearly then, there is an optimum pressure ratio for the cycle.

In the initial sensitivity analyses, ideal turbo-machinery was assumed. Exhibit 4-2 shows the parameters used in the Aspen Plus® simulation of the recuperated cycle.

Exhibit 4-2 Parameters used in Aspen Plus® simulations for recuperated cycle

Parameter	Value
Turbine inlet temperature	1300 °F
Cooler exit temperature	95 °F
Compressor isentropic efficiency	1.0
Turbine isentropic efficiency	1.0
Minimum recuperator temperature approach	10 °F

4.1 Impact of Pressure Ratio

Exhibit 4-3 shows a plot of cycle efficiency versus pressure ratio for the recuperated Brayton cycle with CO_2. Also shown is the corresponding plot for the simple non-recuperated Brayton cycle.

Exhibit 4-3 Cycle efficiency versus pressure ratio for Brayton cycles with CO_2

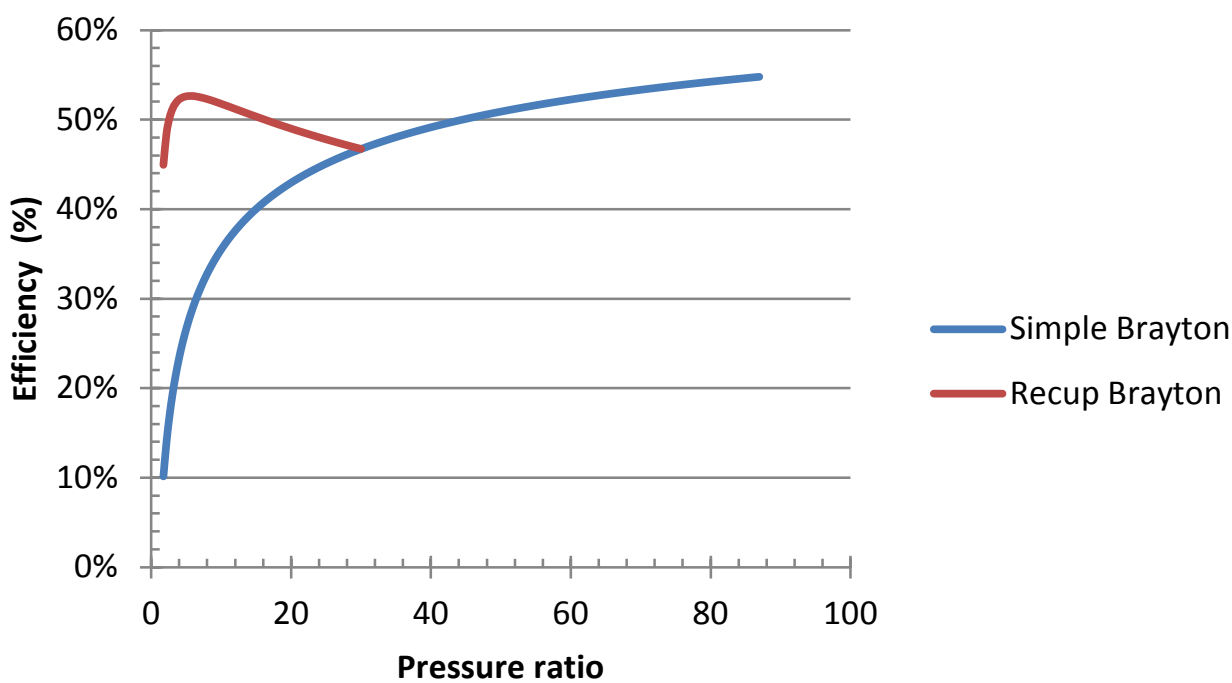

The recuperated cycle shows a much narrower range of operation than the non-recuperated cycle. The maximum cycle pressure ratio occurs at a pressure ratio of approximately 30 when the compressor exit temperature equals the turbine exit temperature and Q_R falls to zero. In the pressure ratio range between 1 and 30, the recuperated cycle efficiency exceeds the non-recuperated cycle efficiency at every pressure. Further, the recuperated cycle shows a maximum in cycle efficiency even for an ideal cycle with ideal turbo-machinery. This maximum occurs at a

relatively low pressure ratio of approximately 5.6. Note the steep drop-off in efficiency for pressure ratios below the point of maximum cycle efficiency.

Exhibit 4-4 shows a plot of specific power versus pressure ratio for recuperated and non-recuperated Brayton cycles with CO_2. The two curves overlay each other, demonstrating that the specific power is unaffected by recuperation.

Exhibit 4-4 Cycle specific power versus pressure ratio for Brayton cycles with CO_2

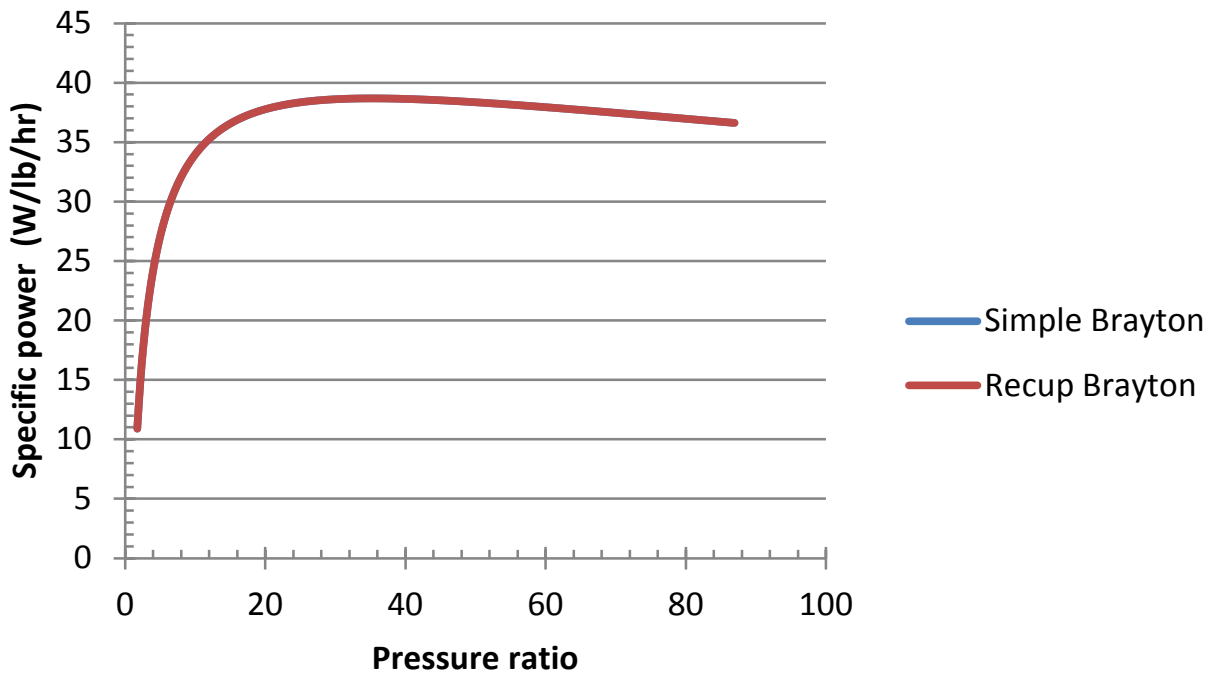

4.2 Analysis of Recuperation

Exhibit 4-5 shows plots of the three cycle heat duties: Q_H, Q_C, and Q_R, as a function of pressure ratio for the recuperated CO_2 Brayton cycle. Exhibit 4-6 depicts the same information as a set of stacked charts. Q_H is a constant for all runs at 100 MMBtu/hr. At the maximum pressure ratio for this recuperated cycle of 30, Q_R becomes zero and no recuperation occurs. As the pressure ratio falls from 30, QC falls slightly and the cycle efficiency increases until the maximum efficiency is reached at a pressure ratio of 5.7. Thereafter, and up to the lower limit of pressure ratio shown, Q_C increases slightly with continued reduction in pressure ratio, and there is a corresponding drop in cycle efficiency.

Exhibit 4-5 Heat duties versus pressure ratio for recuperated Brayton CO_2 cycle

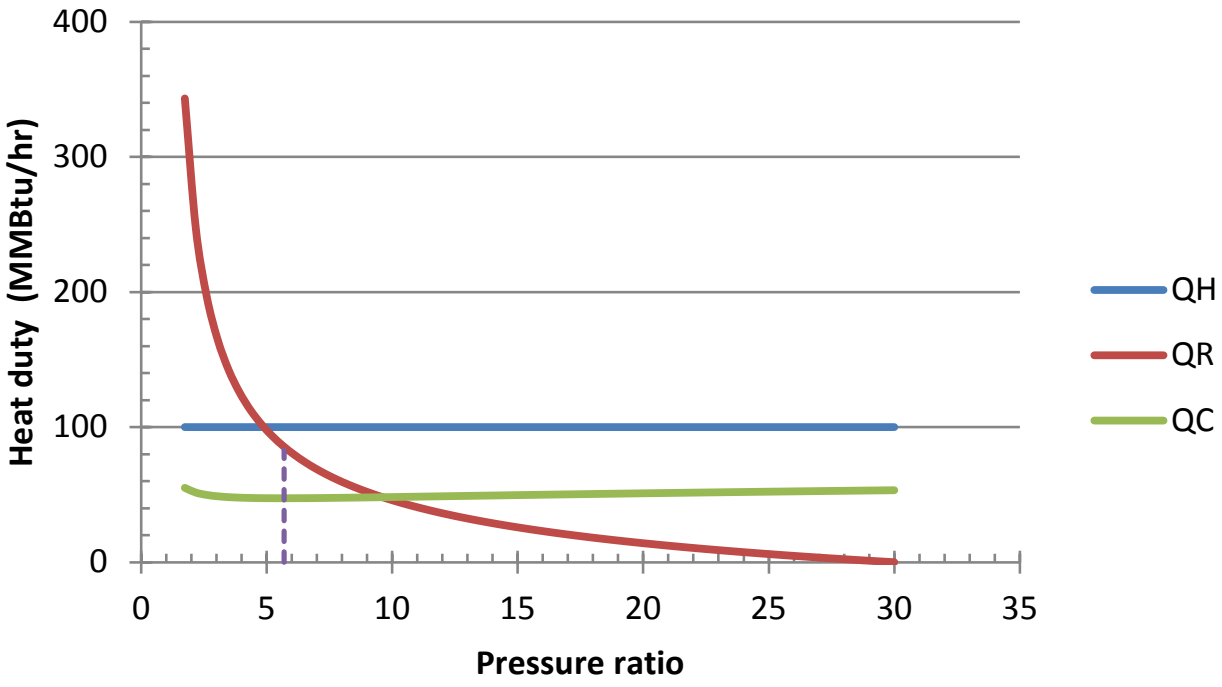

Exhibit 4-6 Heat duties versus pressure ratio for recuperated Brayton CO_2 cycle

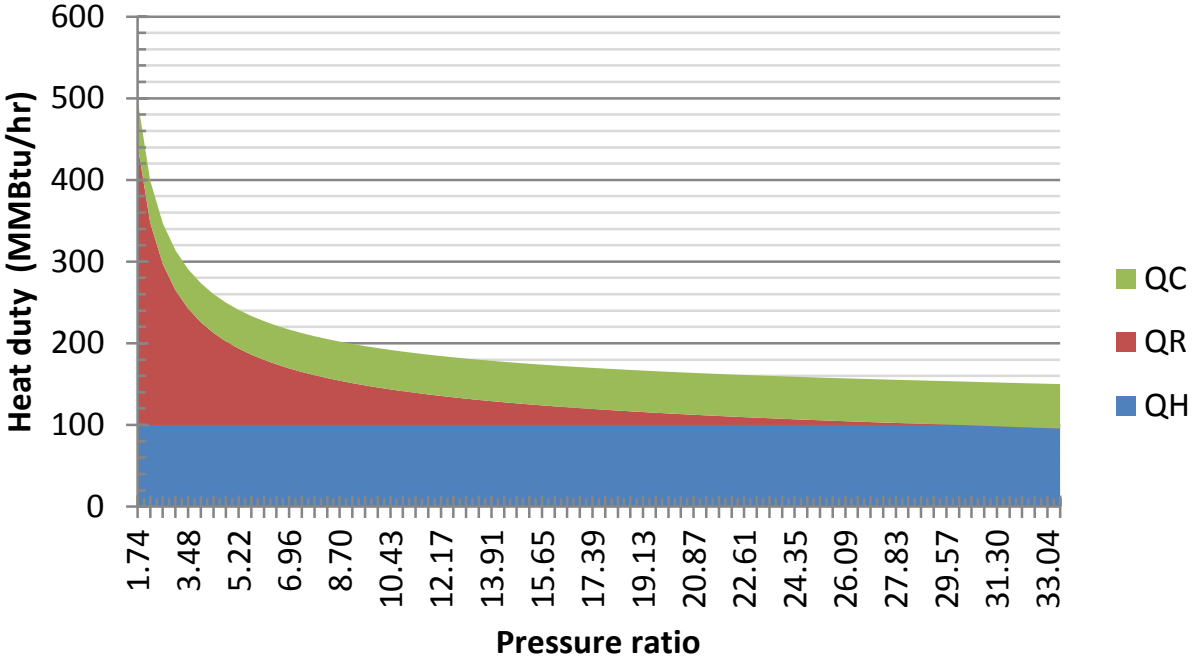

In contract to the modest changes in Q_C, the recuperator duty, Q_R, undergoes an ever increasing and almost exponential rise in magnitude as the pressure ratio falls below 30. At the cycle efficiency maximum, the recuperator heat duty is 86 percent of Q_H. At a pressure ratio below 4.8, Q_R exceeds Q_H.

4.3 Impact of Working Fluid

Exhibit 4-7 shows plots of cycle efficiency versus pressure ratio for CO_2, N_2, and Ar. The curves labeled SB are simple non-recuperated Brayton cycles and the curves labeled RB are recuperated Brayton cycles.

Exhibit 4-7 Cycle efficiency versus pressure ratio for Brayton cycles with CO_2, N_2, and Ar

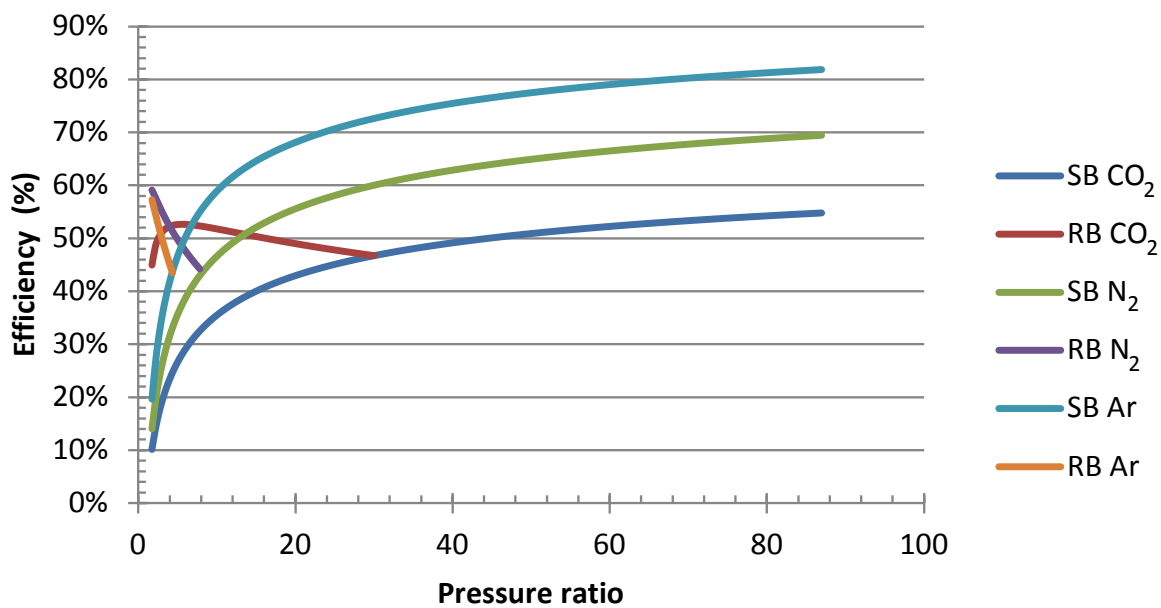

The results show a similar qualitative trend for N_2 and Ar, as they do for CO_2. For N_2, the maximum pressure ratio for a recuperated cycle is 7.8 and the maximum cycle efficiency occurs at a pressure ratio of 1.5. For Ar, the maximum pressure ratio for a recuperated cycle is 4.3, and the maximum cycle efficiency occurs at a pressure ratio of 1.3. At the pressure ratio for maximum efficiency for both N_2 and Ar, Q_R is nearly five times Q_H.

4.4 Impact of Turbine Inlet Temperature

Exhibit 4-8 shows the cycle efficiency versus pressure ratio for a recuperated Brayton CO_2 cycle at eight different settings for the turbine inlet temperature. Also show on this plot is the cycle efficiency for a simple non-recuperated Brayton cycle at a turbine inlet temperature of 1300 °F.

Exhibit 4-8 Impact of turbine inlet temperature for a recuperated Brayton CO_2 cycle

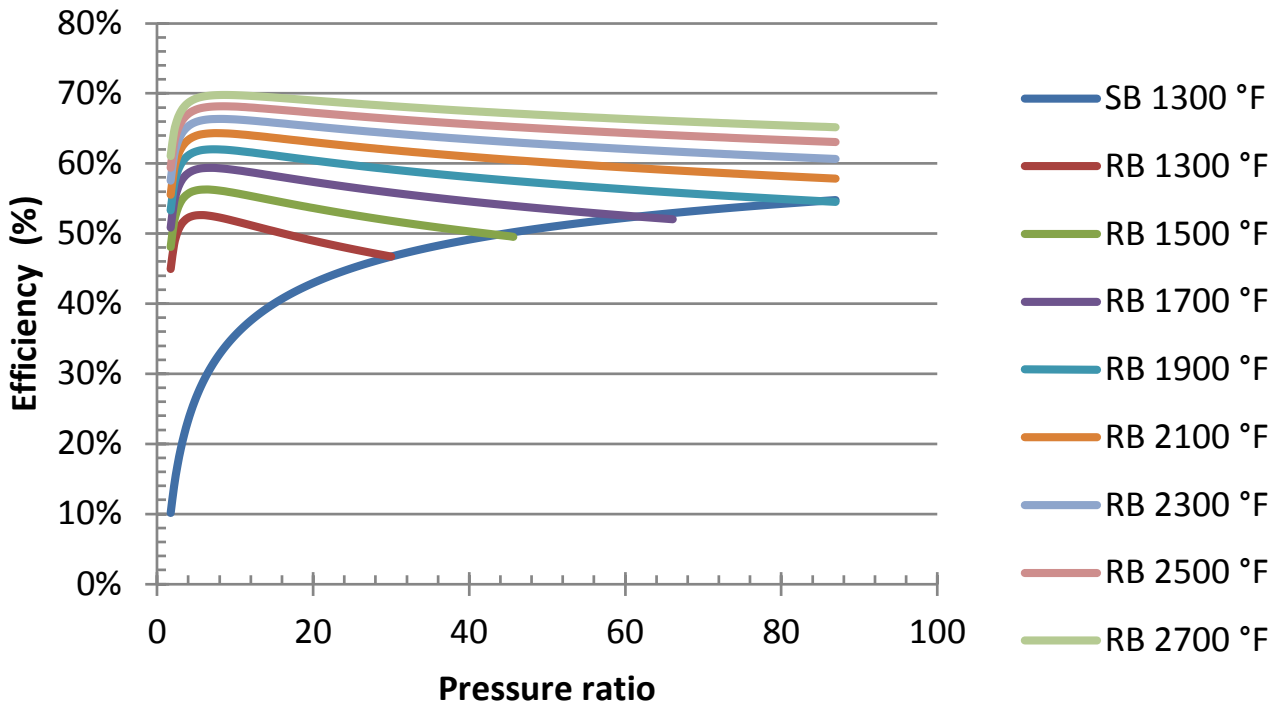

The results show that the cycle efficiency increases monotonically with turbine inlet temperature and that the efficiency increase is proportional to T_2/T_1 (°R). In addition, the pressure ratio for the maximum cycle efficiency increases slightly with increases in turbine inlet temperature. Also of note is that the efficiency versus pressure ratio curve flattens out on the high pressure ratio side of the maximum as the turbine inlet temperature increases.

4.5 Impact of Turbine and Compressor Efficiency

Exhibit 4-9 shows a series of plot pairs for cycle efficiency versus pressure ratio for a CO_2 Brayton cycle at various settings for the turbine and compressor efficiency. Each plot pair shows the efficiency profile for the simple non-recuperated Brayton cycle and the recuperated Brayton cycle. The data for the simple non-recuperated Brayton cycles is the same as shown in Exhibit 2-20. The results confirm the expectation that as the turbo-machinery efficiency drops, the cycle efficiency drops. Note that in the region of low pressure ratio where the cycle efficiency is highest, the decrease in cycle efficiency with decreases in turbo-machinery efficiency is relatively small. For any drop in turbo-machinery efficiency, the drop in cycle efficiency is about one third of what would occur for a non-recuperated cycle operating at peak cycle efficiency.

Exhibit 4-9 Brayton cycle efficiency dependence on turbine and compressor isentropic efficiency

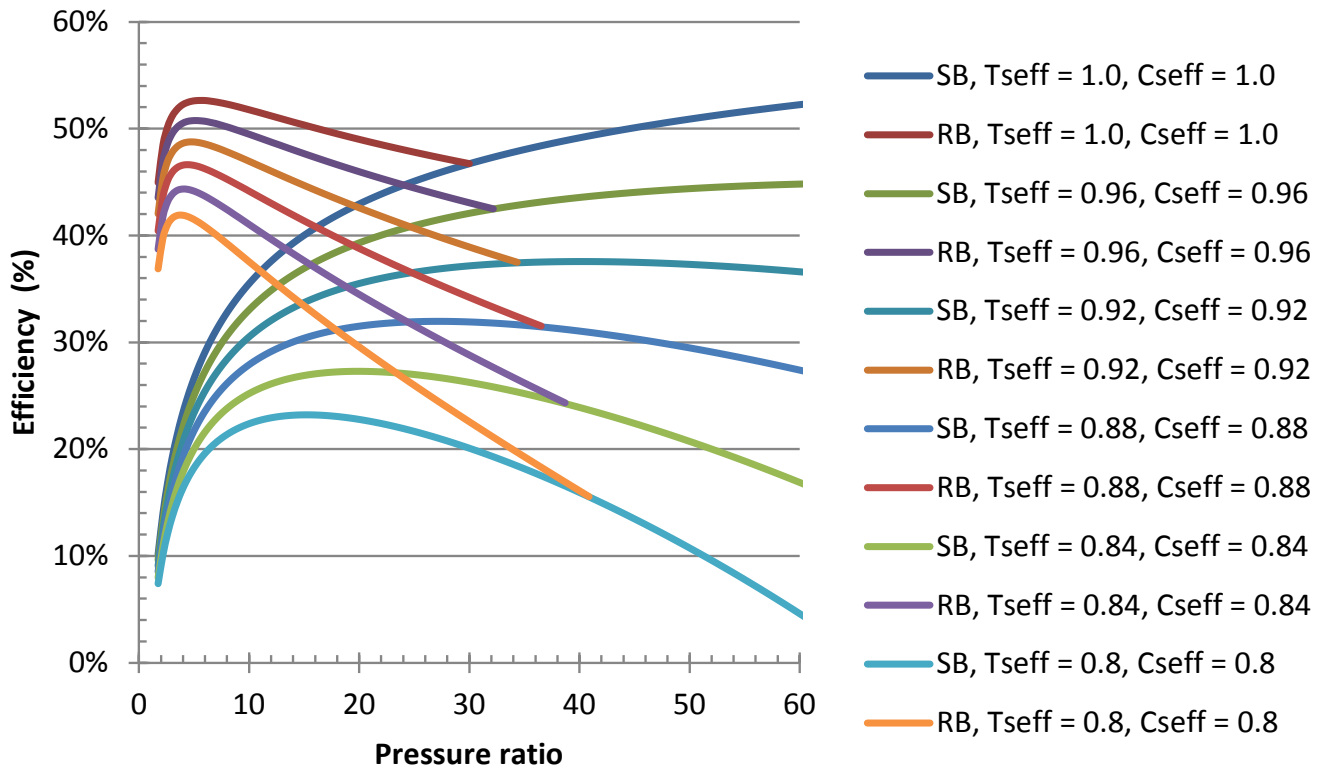

4.6 Impact of Turbine Exit Pressure

As in the case of the non-recuperated cycle, a series of sensitivity runs was performed to examine the dependence of turbine exit pressure on the performance of the recuperated Brayton cycle. Exhibit 4-10 lists the parameters used in the simulation. These are the same values used in the non-recuperated cycle analysis. Exhibit 4-11 shows the impact of turbine exit pressure on the cycle efficiency. This figure shows a markedly different qualitative trend compared to Exhibit 2-23. At a turbine exit pressure of 100 psia, there is a maximum in cycle efficiency at a pressure ratio of 1.5. As the turbine exit pressure increases towards the CO_2 critical pressure, the maximum cycle efficiency decreases and the maximum in the efficiency versus pressure ratio curve moves to slightly higher pressure ratios. At turbine exit pressures of 900 psia and higher, the curves flatten out in the low pressure ratio region and the pressure ratio at maximum cycle efficiency starts to increase more rapidly. At a turbine exit pressure of 1200 psia and above, the cycle efficiency versus pressure ratio curve does not vary with turbine exit pressure.

Exhibit 4-10 Parameters used in Aspen Plus® simulations

Parameter	Value
Turbine inlet temperature	1300 °F
Cooler exit temperature	95 °F
Compressor isentropic efficiency	0.85
Turbine isentropic efficiency	0.927
Minimum recuperator temperature approach	10 °F

Exhibit 4-11 Recuperated Brayton cycle efficiency dependence on turbine exit pressure (psia)

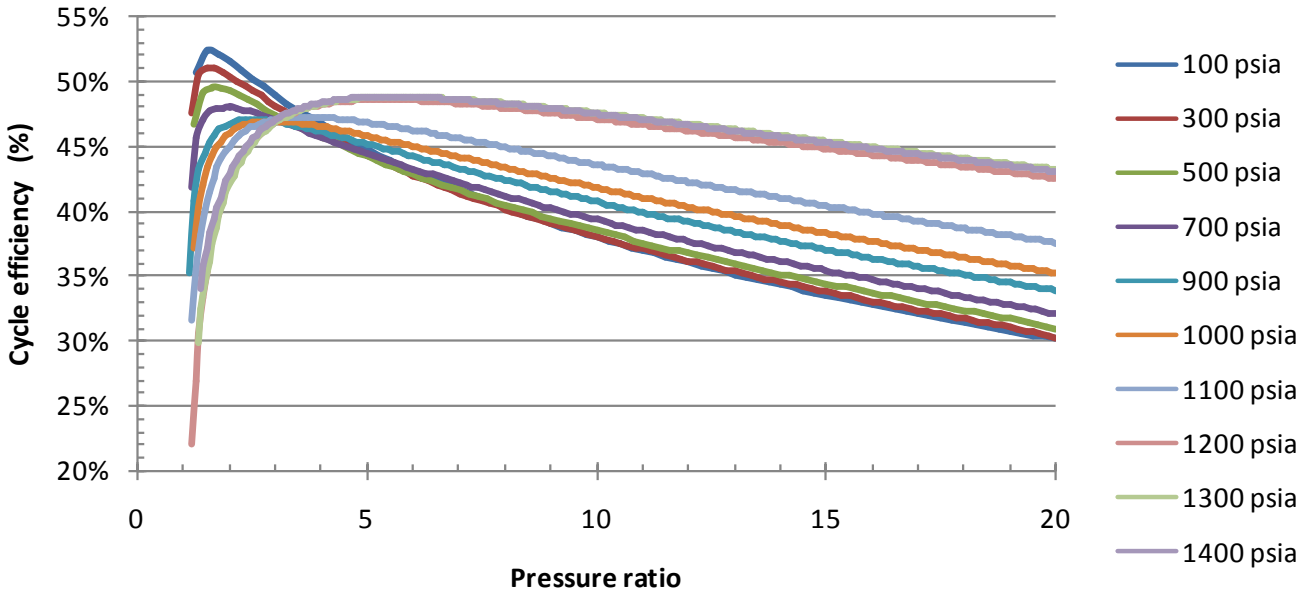

The reason that the cycle efficiency is highest for low cycle pressures is due to the effectiveness of the recuperator at low pressure. The effectiveness for the recuperator is defined as the ratio of the cold-side temperature rise to the hot-side temperature drop. Exhibit 4-12 shows a plot of recuperator effectiveness as a function of pressure ratio for the same selections of turbine exit pressure, as shown in Exhibit 4-11. The cycle efficiency should increase with increasing recuperator efficiency, all other things being equal, and a higher recuperator effectiveness will allow more effective use of the hot source heat, allow a greater CO_2 flow, and lead to a higher net cycle output. The results shown in Exhibit 4-11 are fully consistent with this trend. In a non-recuperated cycle, the cycle efficiency increases as the turbine exit pressure increases for a low value such as 100 psia. This was concluded to be due to the changes in CO_2 properties as the working fluid spent a larger fraction of its path as a supercritical fluid. This phenomenon still occurs in the recuperated cycle but it is offset by the effects of the recuperator effectiveness and the higher heat recovery possible in the low pressure recuperator.

Exhibit 4-12 Recuperator effectiveness as a function of pressure ratio

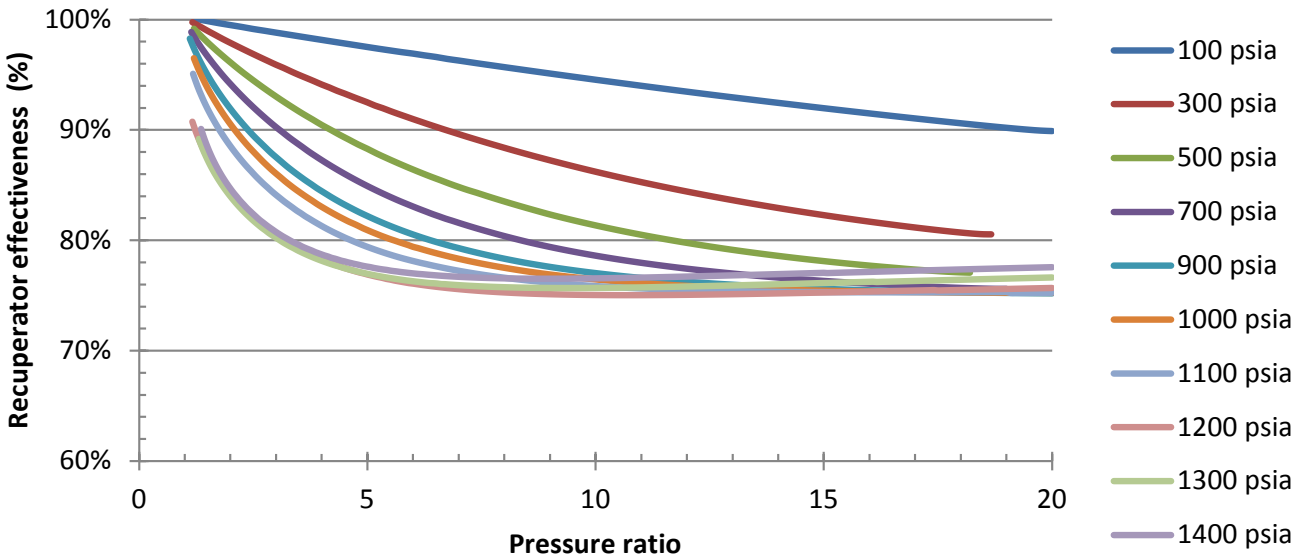

While these results indicate the maximum cycle efficiency for a recuperated Brayton CO_2 cycle occurs with small cycle pressures and very small pressure ratios. However, this does not reflect practical operation. Exhibit 4-13 shows a plot of specific power versus pressure ratio for the same turbine exit pressures as shown in Exhibit 4-12. For any turbine exit pressure, the specific power is very low for a very low pressure ratio cycle (PR < 2). Beyond a pressure ratio of 5, the specific power rises slowly to its maximum value. As the turbine inlet pressure rises from 100 psia, the specific power increases until the turbine exit pressure reaches 1200 psia. Further increases in turbine exit pressure beyond 1200 psia have very little impact on the cycle-specific power.

Based on these results, it appears that a practical recuperated Brayton cycle would operate at a turbine exit pressure of approximately 1200 psia and a pressure ratio in the range of 5 to 10.

The variation in recuperator effectiveness shown in Exhibit 4-12 is a result of the high c_p of CO_2 in the region of the critical point. This has a more pronounced effect on the cold side of the Brayton cycle loop than on the hot side. The mismatch in thermal capacitance of the streams limits the benefits of recuperation. This can be partially ameliorated by adjusting the configuration on the recuperated Brayton cycle. This will be explored in the next section.

Exhibit 4-13 Recuperated Brayton cycle-specific power dependence on turbine exit pressure

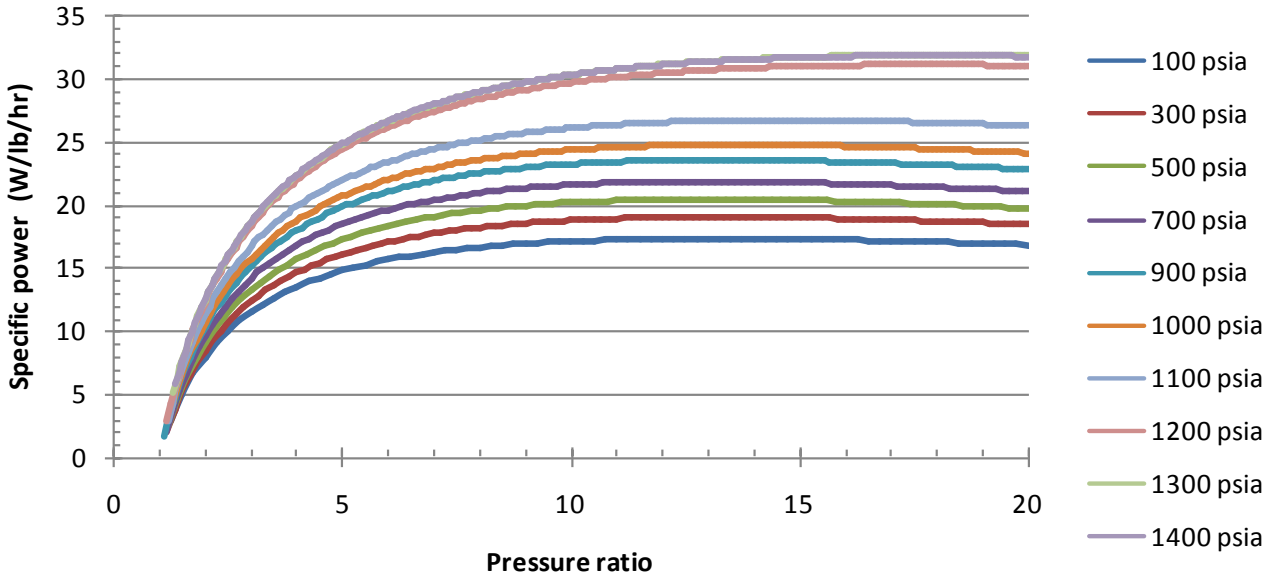

5 Two-stage Recuperated (Recompression) Brayton Cycle

Exhibit 5-1 shows a BFD for a slightly more complex variant of the Brayton cycle. Compared to the single-stage recuperation cycle, this cycle can be seen to have a split two-stage recuperator with each stage having a different cold-side CO_2 flow rate. The hot-side CO_2 stream passes through both recuperator stages. After exiting the recuperator, the hot-side stream is split with a portion following the same path as a simple Brayton cycle and the other bypassing the CO_2 cooler and directly entering a second compressor at point I on Exhibit 5-1.

For the initial analysis of the cycle, pressure drops are neglected. Since the feed stream to the main compressor (point A) has a lower temperature than the feed stream to the secondary compressor (point I) and since the pressure change in both compressors is the same, the specific power for the secondary compressor will be higher than that for the main compressor. Further, the stream exiting the secondary compressor will be at a higher temperature than the stream exiting the main compressor.

A degree of freedom in the configuration is the fraction of the hot-side CO_2 that is diverted away from the CO_2 cooler and enters the secondary compressor. With a split of zero, the cycle reverts to the simple recuperated Brayton cycle. As the split increases, the temperature of the cold-side stream entering the first stage recuperator will increase. At some point, a minimum temperature approach will be reached indicating the maximum amount of split possible.

The overall impact of the stream splitting is to raise the effectiveness of the recuperator. This will be explored in detail in the following section.

Exhibit 5-1 Two-stage recuperated (recompression) Brayton cycle

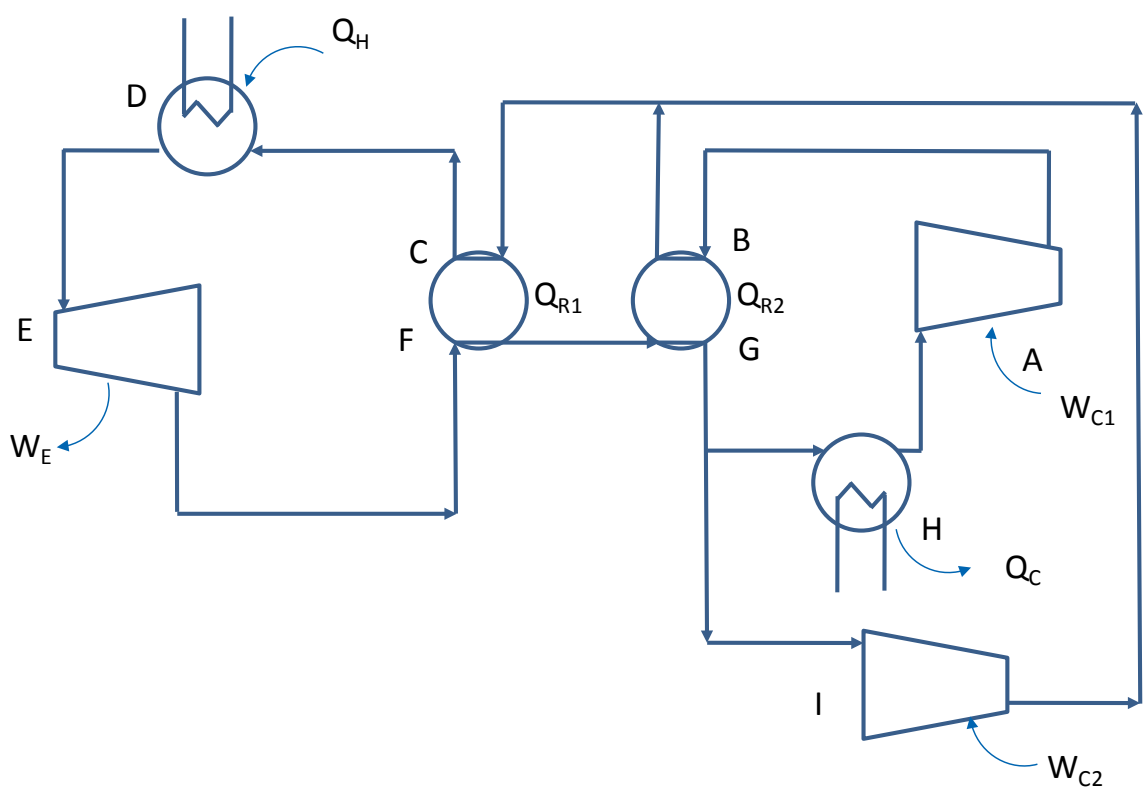

5.1 Impact on Recuperator Effectiveness

In the case of zero split of the hot-side recuperator effluent, the minimum temperature approach always occurs at the hot-side exit and cold-side entrance (points G and B, respectively in Exhibit 5-1). Exhibit 5-2 is a temperature-enthalpy diagram for the CO_2 Brayton cycle operated with the parameters listed in Exhibit 4-2 and a pressure ratio of 1.74. The region between the dashed vertical lines is the recuperator region. To the left of the recuperator region is the CO_2 cooler and to the right is the hot source. At the low-temperature end of the recuperator, the approach temperature is 10 °F. At this point the cold-side temperature-enthalpy plot has a relatively small slope reflecting the high c_p of the CO_2. Moving towards the high temperature end, the temperature difference in the recuperator increases. This increase is rapid at first and then asymptotes towards the maximum value at the high-temperature end of the recuperator. It is this effect that reduces the recuperator effectiveness.

When CO_2 diverts through the secondary compressor loop, it bypasses the cooler and decreases the thermal capacitance of the cold-side CO_2. This decreases the cold-side temperature-enthalpy curve slope and decreases the temperature difference between the hot and cold sides of the recuperator, particularly the maximum temperature difference and the high temperature end of the recuperator. Reducing this temperature difference allows more CO_2 to pass through the cycle for the same heat input, raising cycle output and efficiency. Exhibit 5-3 shows the temperature-enthalpy diagram for this system when the cooler bypass split fraction is 0.37. This is the maximum amount of bypass that can occur subject to the 10 °F minimum approach temperature. Compared to Exhibit 5-2, the maximum temperature approach in the bypass case has been reduced from 131 °F to 66 °F and the recuperator effectiveness has increased from 0.824 to 0.885.

Exhibit 5-2 Temperature-enthalpy diagram for the recuperated Brayton cycle

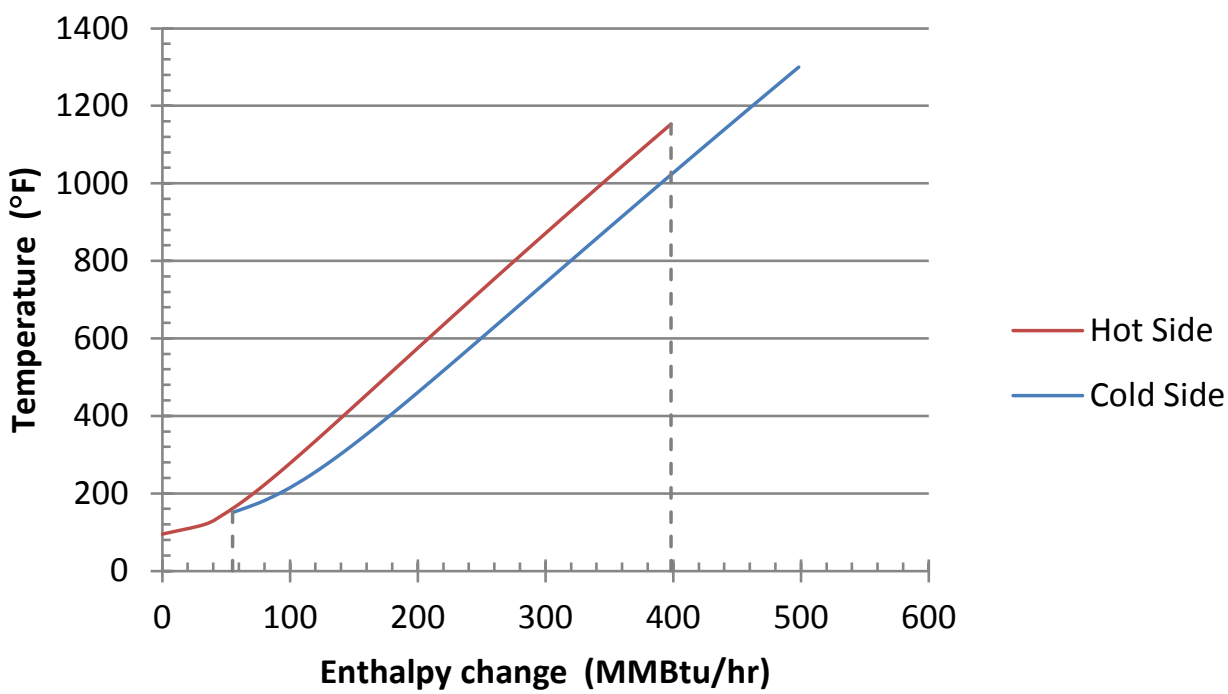

Exhibit 5-3 Temperature-enthalpy diagram for the recompression Brayton cycle, bypass = 0.37

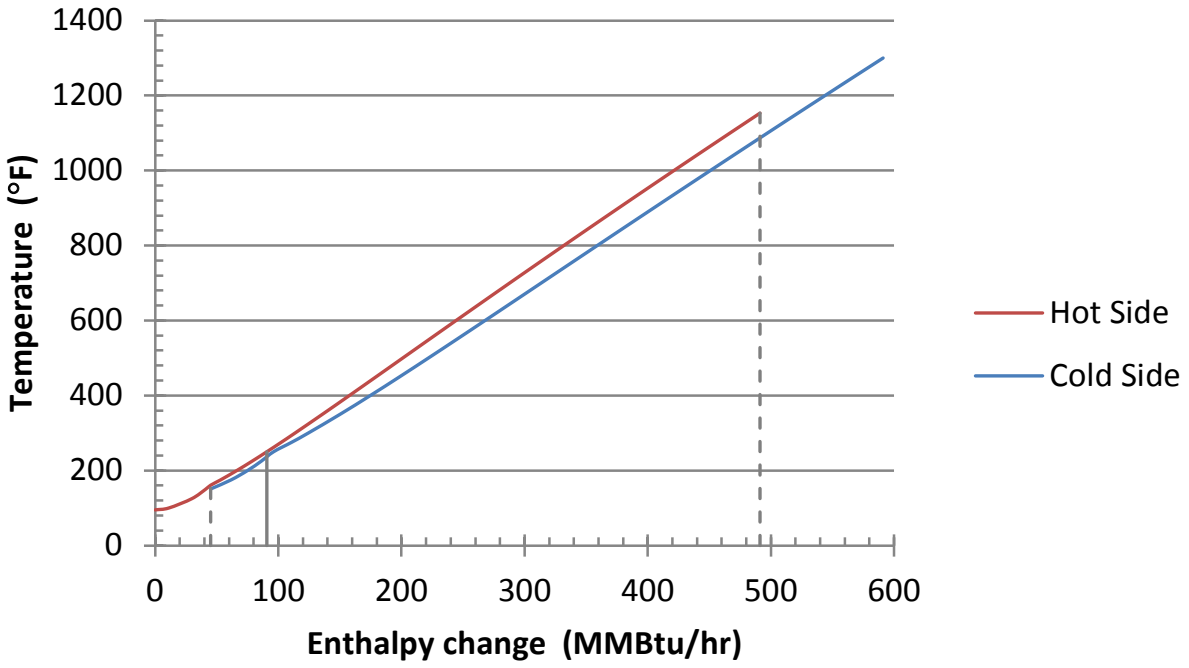

Exhibit 5-4 shows the cycle efficiency versus cooler bypass split fraction for this system. The increase in cycle efficiency is approximately 10 percentage points. As will be shown in the following section, a 10 percentage point efficiency increase with a recompression cycle is exceptionally large.

Exhibit 5-4 CO_2 recompression Brayton cycle efficiency versus cooler bypass fraction

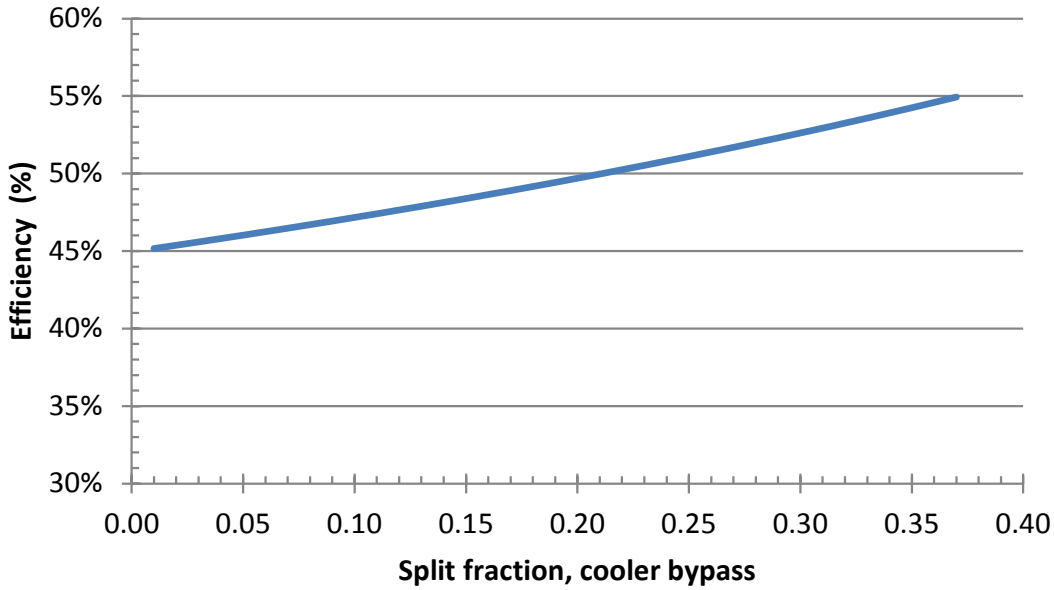

5.2 Impact of Pressure Ratio

Exhibit 5-5 shows the recompression Brayton cycle efficiency versus cycle pressure ratio. At each pressure ratio, the cooler bypass was adjusted to maximize the cycle efficiency. The corresponding bypass fractions are also shown on Exhibit 5-5 as is the cycle efficiency for a simple recuperated Brayton cycle, i.e., when the cooler bypass is zero.

For both the recompression Brayton cycle and the simple recuperated Brayton cycle, the cycle efficiency shows a maximum at some pressure ratio. This maximum is greater in the recompression cycle and occurs at a lower pressure ratio.

Exhibit 5-5 Impact of cycle pressure ratio on the recompression Brayton cycle efficiency

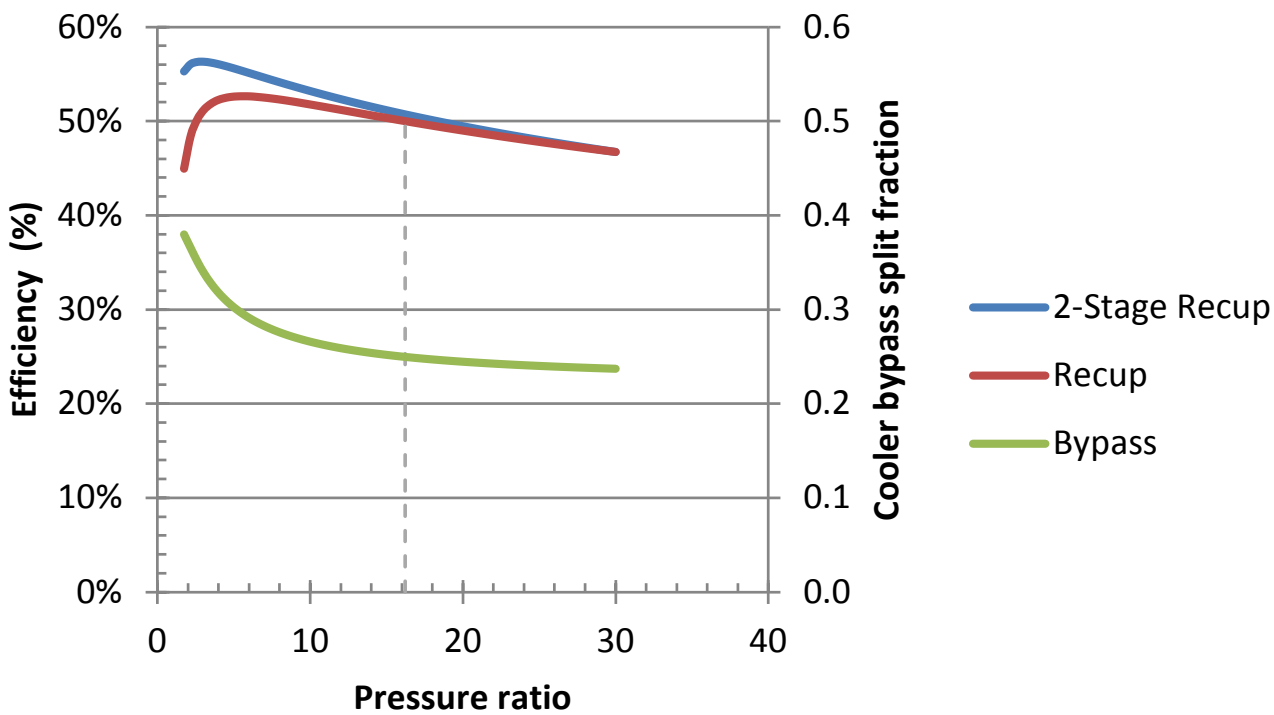

Exhibit 5-5 shows that the recompression Brayton cycle has a higher efficiency than a simple recuperated Brayton cycle for pressure ratios under 16. The effect is particularly significant for low pressure ratios below 6. This result is not surprising. At even moderate pressure ratios, the compressor exit temperature is high enough that the CO_2 will not exhibit supercritical fluid behavior. The thermal capacitance of the cold-side is nearly equal to that of the hot-side and no significant improvement in recuperator effectiveness can be attained through cooler bypass.

5.3 Impact of Turbine Inlet Temperature

Exhibit 5-6 shows the recompression Brayton cycle efficiency versus pressure ratio curves for eight different settings for the turbine inlet temperature. For each turbine inlet temperature, the corresponding plot for the simple recuperated Brayton cycle is also shown. All of the efficiency versus pressure ratio plot pairs show the same qualitative trends as shown in Exhibit 5-5. The recompression cycle efficiency is greater than the recuperated cycle efficiency for each plot pair.

This effect is greatest at the lowest pressure ratios and diminishes as the pressure ratio increases. As the turbine inlet temperature increases, the recompression cycle efficiency increases at any pressure ratio. As the turbine inlet temperature increases, the maximum recompression cycle efficiency increases and the drop off in efficiency at pressure ratios above the efficiency maximum diminishes. This means that the sensitivity of the cycle efficiency to pressure ratio decreases as the turbine inlet temperature increases.

Exhibit 5-6 Impact of turbine inlet temperature for a recuperated Brayton CO_2 cycle

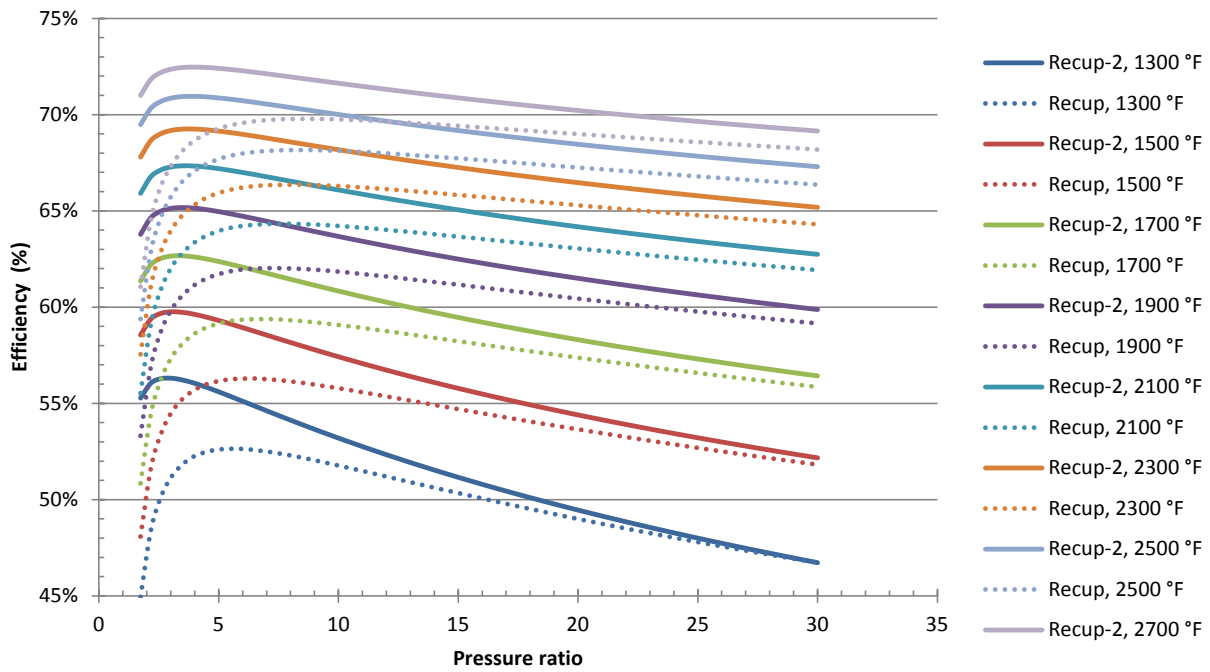

5.4 Impact of Turbine and Compressor Efficiency

A sensitivity run of cycle efficiency versus pressure ratio was executed on a recompression Brayton cycle using the parameters shown in Exhibit 4-10. The results are shown in Exhibit 5-7. The recompression and recuperated cycles are shown as a plot pair. Also shown is the corresponding cooler bypass fraction for the recompression cycle. The results in Exhibit 5-5 for the case with ideal turbo-machinery are shown in Exhibit 5-7 as the dark gray plot pair.

With the lower turbine and compressor efficiency, the cycle efficiency decreases as expected. As with the recuperated Brayton cycle, lowering the turbo-machinery efficiencies shifts the maximum cycle efficiency slightly towards a lower pressure ratio (from 4.2 to 2.5). Two other impacts are notable. The lowering of the turbo-machinery efficiencies increases the rate of efficiency drop off when operating at a pressure ratio other than a maximum cycle efficiency. This means that the recompression cycle has been made more sensitive to deviations in the pressure ratio. Another notable impact from the lowered turbo-machinery efficiencies is that the efficiency curves have a crossover point around a pressure ratio of 16. At pressure ratios above this level, the recompression cycle actually has a lower efficiency than the simple recuperated Brayton cycle.

Exhibit 5-7 Impact of turbine and compressor efficiency on recompression Brayton cycle efficiency

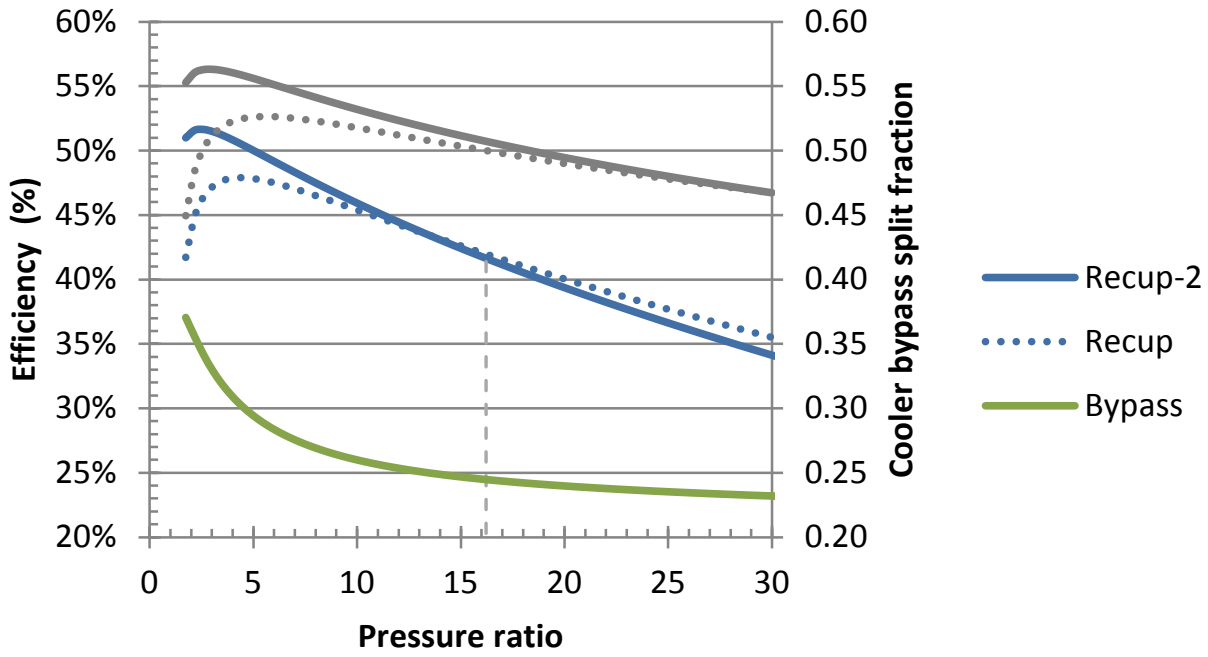

5.5 Impact of Turbine Exit Pressure

Exhibit 5-8 shows the variation in cycle efficiency versus pressure ratio at 14 different settings for the turbine exit pressure (Pex). The dependence on turbine exit pressure is similar to what was observed for the non-recuperated Brayton cycle. At low cycle pressures with turbine exit pressure in the range of 400 to 800 psia, the efficiency versus pressure ratio plot shows no dependence on turbine exit pressure. As the turbine exit pressure increases beyond 800 psia, the efficiency increases at any pressure ratio. This effect continues until the turbine exit pressure reaches approximately 1300 psia. As the turbine exit pressure increases beyond this value, the trend reverses and the cycle efficiency decreases with increasing turbine exit pressure.

Exhibit 5-8 Recompression Brayton cycle efficiency dependence on turbine exit pressure (psia)

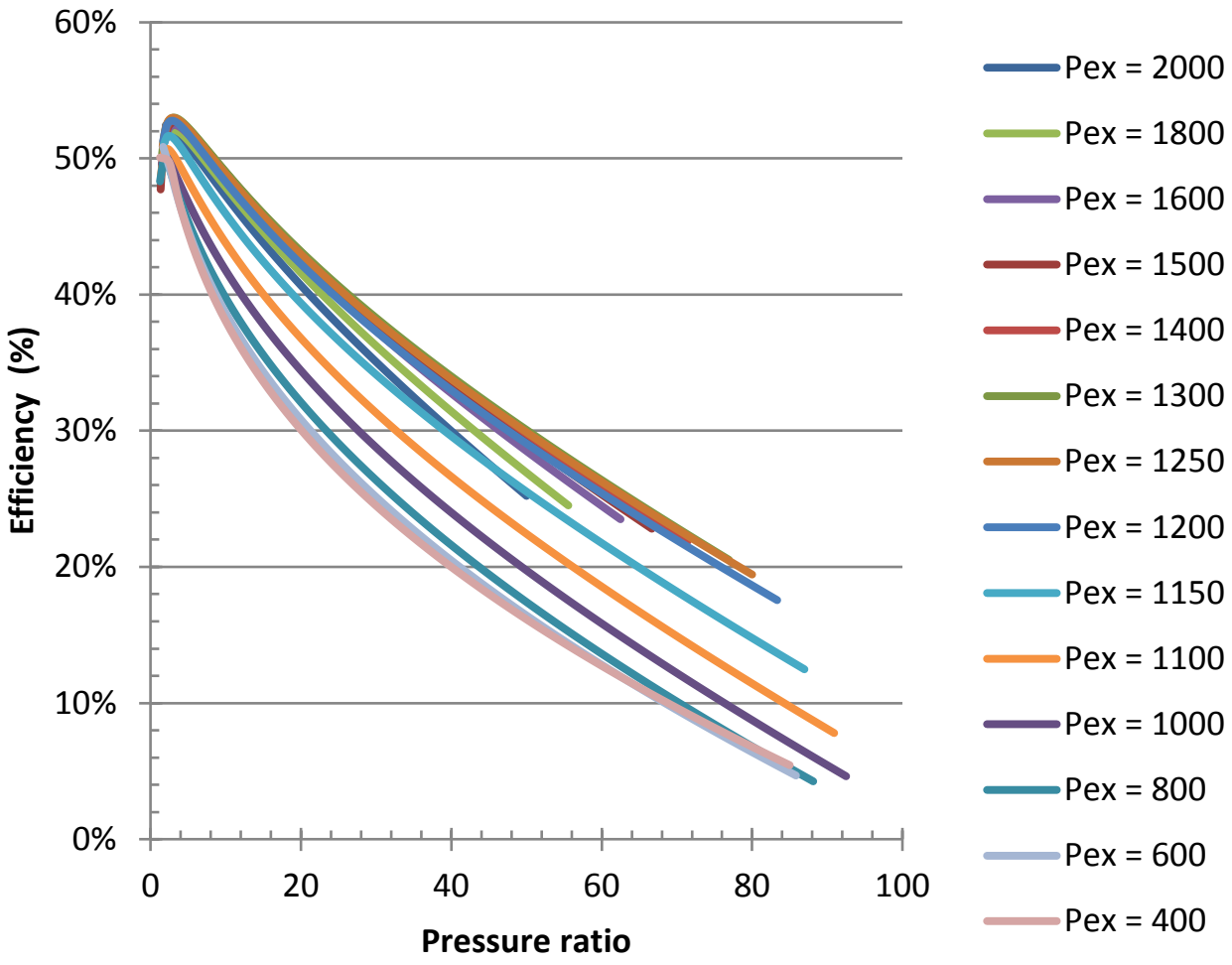

Exhibit 5-9 is a plot of the maximum cycle efficiency versus turbine exit pressure. The maximum cycle efficiency of 53 percent occurs at a turbine exit pressure of 1300 psia. Of note is the sharp drop off in efficiency when the turbine exit pressure falls below 1250 psia. The maximum cycle efficiency drops approximately 2.2 percentage points with a 150 psia drop in turbine exit pressure. This suggests that if pressure drops are included in the analysis, the maximum cycle efficiency will be relatively sensitive to the value of the pressure drop.

Exhibit 5-10 shows a plot of specific power versus pressure ratio for the same settings of turbine exit pressure as used in Exhibit 5-9. As the turbine exit pressure increases up to 1200 psia, the specific power increases at any pressure ratio. Between turbine exit pressures of approximately 1200 to 1600 psia, there is little variation in specific power with turbine exit pressure. As the turbine exit pressure increases beyond 1600 psia, the specific power decreases. The specific power shows a maximum at a moderate pressure ratio for all values of turbine exit pressure shown in Exhibit 5-10. The peak specific power occurs in the pressure ratio range of 12 to 16. This is significantly higher than the pressure ratio range for maximum cycle efficiency and suggests that the economic optimum will lie in between those ranges.

Exhibit 5-9 Maximum recompression Brayton cycle efficiency versus turbine exit pressure

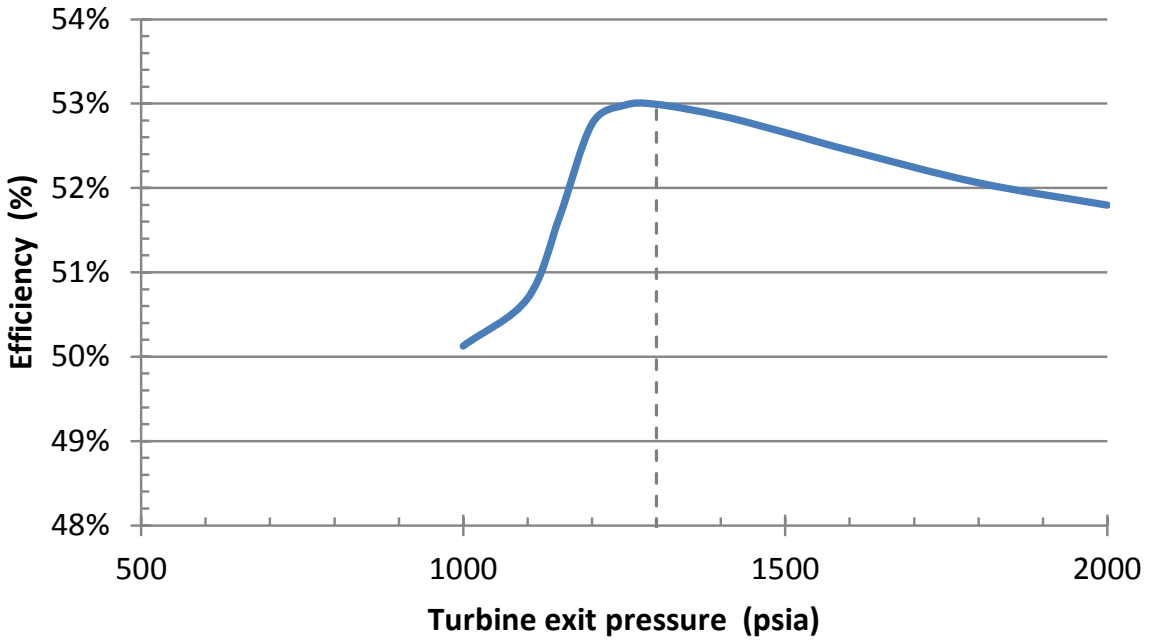

Exhibit 5-10 Recompression Brayton cycle-specific power dependence on turbine exit pressure

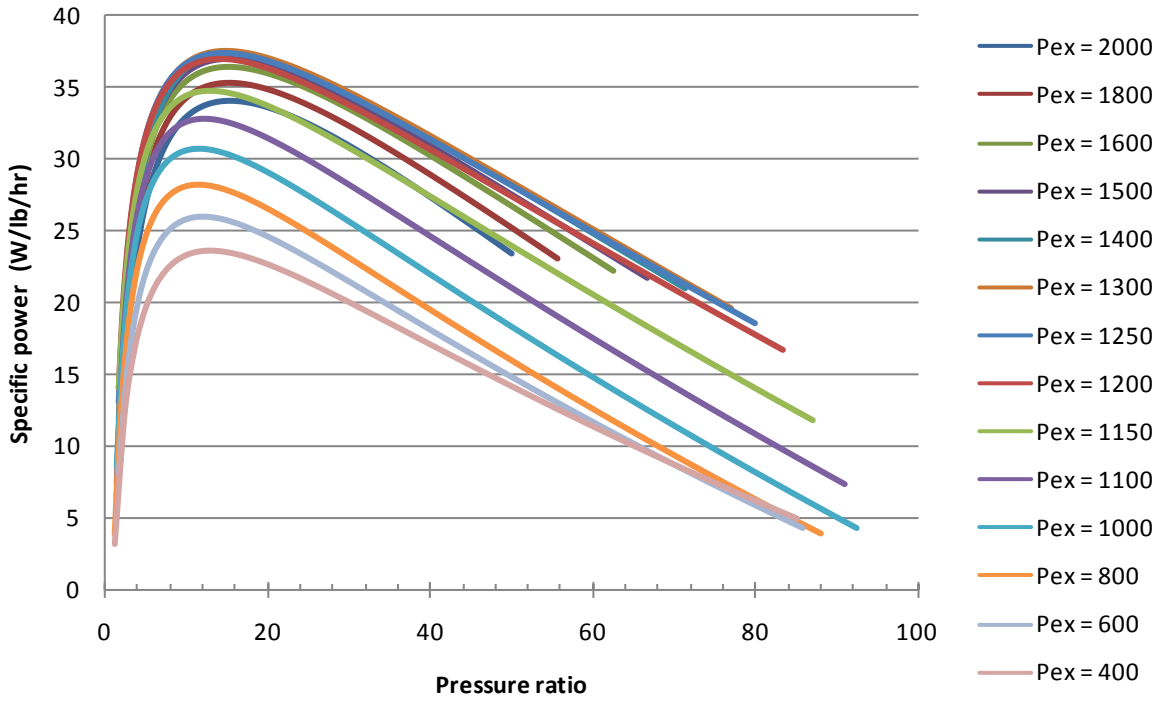

5.6 Impact of Working Fluid

The improvement in process efficiency resulting from the two-stage recuperator occurs because the latter configuration can mitigate the difference in thermal capacitance in CO_2 that occurs between the hot-side and cold-side. It is because of the non-ideal behavior of CO_2 in the critical region that the cold-side thermal capacitance is significantly greater than the hot-side thermal capacitance. Hence, it is not expected that the recompression cycle will yield significant benefits when applied to N_2 or Ar cycles. This expectation is confirmed in the results shown in Exhibit 5-11. The cycle efficiency dependence on pressure ratio does not change when recompression is introduced for both N_2 and Ar.

Exhibit 5-11 Recompression Brayton cycle efficiency versus pressure ratio for N_2 and Ar

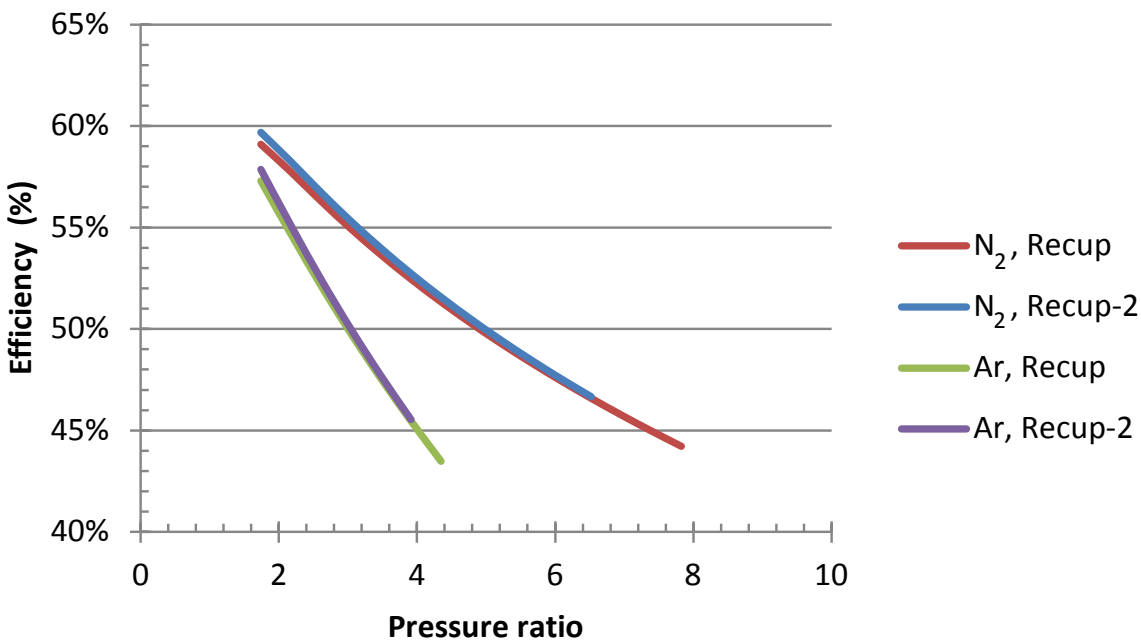

6 Recompression Brayton Cycle with Reheat

Exhibit 6-1 shows a BFD for a slightly more complex variant of the recompression Brayton cycle. The turbine section has been split into two turbines such that the pressure ratio of expansion is the same for both turbines. The exhaust from turbine 1 is reheated using the same hot source such that the inlet temperature to turbine 2 is the same as the inlet temperature to turbine 1.

Exhibit 6-1 Two-stage recuperated (recompression) Brayton cycle with reheat

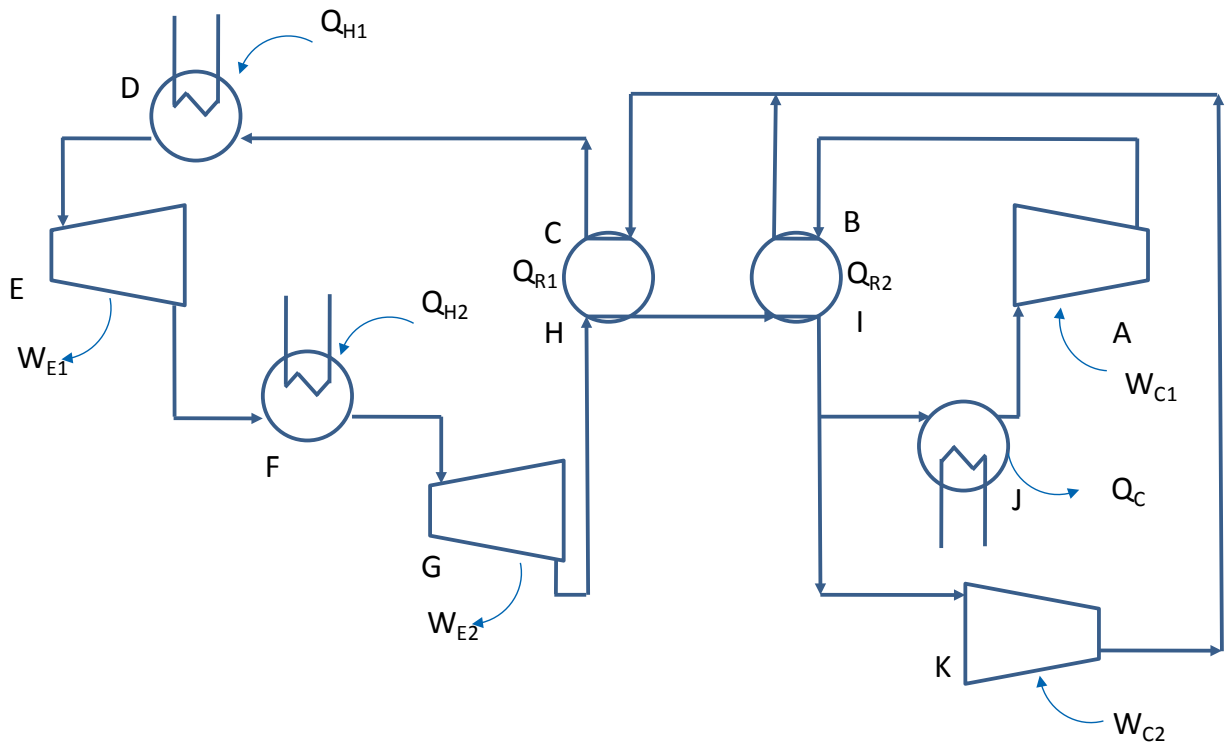

6.1 Impact of Pressure Ratio

Exhibit 6-2 shows a plot of cycle efficiency versus pressure ratio for the recompression reheat Brayton cycle with CO_2. Also shown is the corresponding efficiency versus pressure ratio curves for the recompression Brayton cycle and the recuperated Brayton cycle. Using reheat boosts the cycle efficiency at every pressure ratio. The pressure ratio at the maximum efficiency increases from approximately 3 in the recompression Brayton cycle to approximately 4 in the recompression reheat Brayton cycle. The maximum efficiency in the recompression reheat Brayton cycle is approximately 1.5 percentage points greater than for the recompression Brayton cycle. Also, the reheat cycle shows a significantly lower drop off in efficiency at higher pressure ratios than is observed for the recompression Brayton cycle.

Exhibit 6-2 Cycle efficiency versus pressure ratio for the recompression reheat Brayton cycle

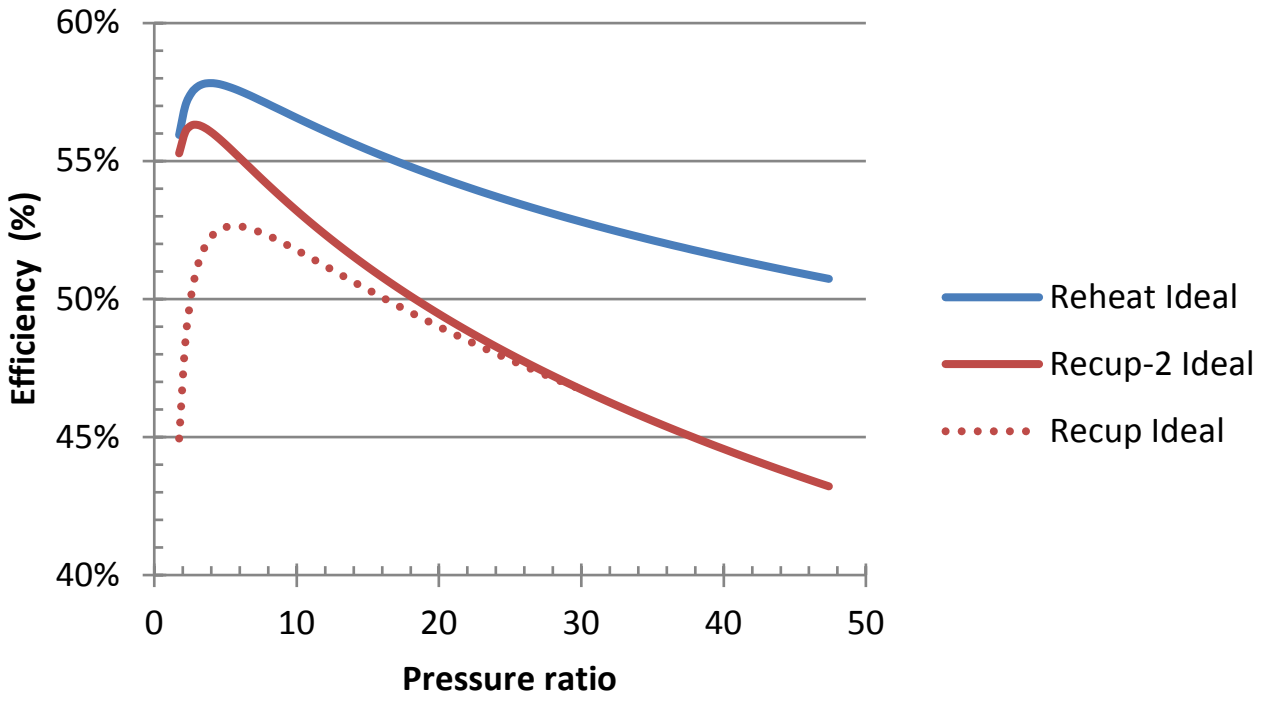

6.2 Impact of Turbine and Compressor Efficiency

A sensitivity run of cycle efficiency versus pressure ratio was executed on a recompression reheat Brayton cycle using the parameters shown in Exhibit 4-10. The results are shown in Exhibit 6-3. The recompression and recuperated cycles are shown as a plot pair. The results in Exhibit 6-2 for the case with ideal turbo-machinery are shown in Exhibit 6-3 as the gray plots.

The main impact of the lowered turbo-machinery efficiencies is to lower the cycle efficiency. In addition, the efficiency versus pressure ratio curve for the recompression reheat Brayton cycle has a sharper maximum occurring at a lower pressure ratio, and a greater sensitivity to pressure for cycles with non-ideal turbo-machinery.

Exhibit 6-3 Impact of turbine and compressor efficiency on recompression reheat Brayton cycle efficiency

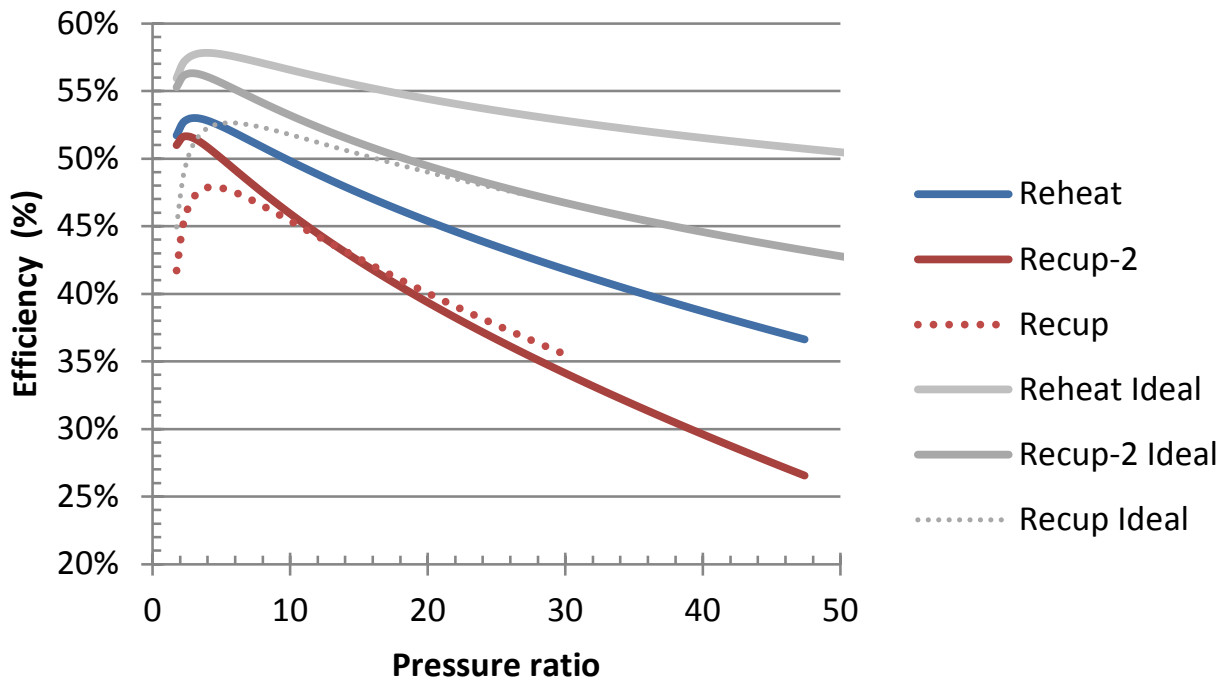

Exhibit 6-4 shows the specific power for the recompression reheat Brayton cycle as a function of pressure ratio. The results are similar to those seen for the recompression Brayton cycle without reheat. The specific power shows a maximum at a moderate pressure ratio which is considerably higher than the pressure ratio at which the maximum cycle efficiency occurs. Note that for a recompression cycle with reheat, the sensitivity of the specific power to pressure ratio is significantly less than for a recompression cycle without reheat.

Exhibit 6-4 Recompression reheat Brayton cycle-specific power dependence on pressure ratio

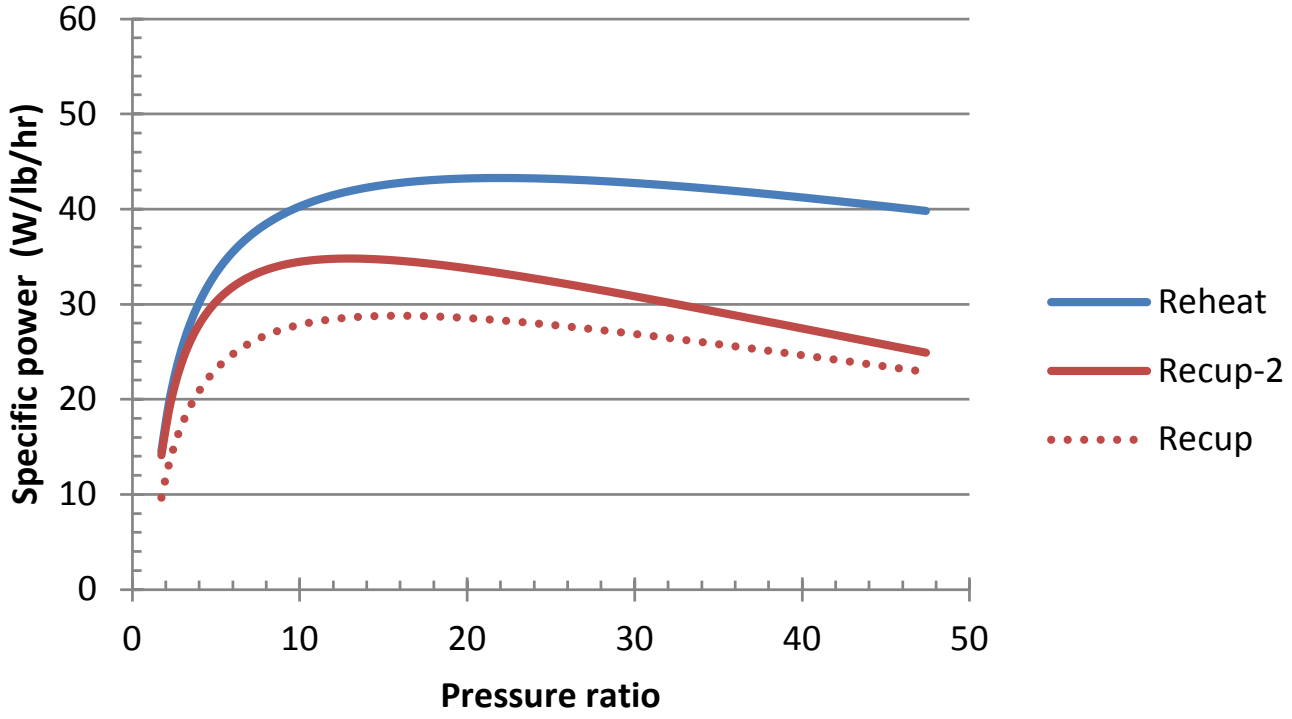

7 Conclusions

The non-recuperated Brayton cycle is the simplest form of the closed Brayton cycle. For ideal conditions (adiabatic operation, turbo-machinery efficiencies of 1 and no pressure drops), the cycle efficiency increases monotonically with pressure ratio and shows no dependence on turbine inlet temperature. For non-ideal cycles and working fluids, the cycle efficiency increases with turbine inlet temperature and at any given turbine inlet temperature, shows a maximum at some pressure ratio. The cycle efficiency decreases as either the turbine efficiency or compressor efficiency decreases but the impacts of drops in the turbine efficiency are more significant. The cycle-specific power dependence on pressure ratio shows a maximum that occurs at a lower pressure ratio than the cycle efficiency maximum. The cycle efficiency is greatest for working fluids with the largest value of γ. However, the specific power is greatest for the working fluids with the greatest density and this favors CO_2 when the cycle conditions are such that CO_2 exhibits properties of a supercritical fluid. For the CO_2 Brayton cycle, the cycle efficiency is dependent on cycle pressure. This can best be seen by the sensitivity of cycle efficiency to the turbine exit pressure, which is the minimum cycle pressure if pressure drops are not considered. For the CO_2 Brayton cycle, a maximum in efficiency occurs at a turbine exit pressure of approximately 1200 psia, which is just above the CO_2 critical pressure.

Near the critical region, the physical properties of CO_2 are highly non-ideal and highly non-linear. Variations in c_p, γ, and density are very large in this region and it is essential that the equation of state used to estimate the physical properties of the working fluid capture this behavior to accurately estimate cycle performance. In this work, it was found that the PR-BM equation of state in Aspen Plus® was able to estimate the properties of CO_2 to an acceptable level of accuracy.

Introducing a recuperator in the Brayton cycle, in which a portion of the sensible heat in the turbine exhaust is used to preheat the working fluid prior to entering the hot source, increases the cycle efficiency at every pressure ratio for which recuperation is feasible. The recuperated Brayton cycle shows a maximum in cycle efficiency that occurs at a much lower pressure ratio than for a non-recuperated cycle. Recuperation acts to increase cycle efficiency by sparing the hot-source heat duty and allowing more working fluid to enter the cycle. For an ideal cycle, recuperation has no impact on specific power. In the non-recuperated Brayton cycle, efficiency is not dependent on turbine inlet temperature but there is a strong dependence on turbine inlet temperature seen in the recuperated Brayton cycle. As in the non-recuperated cycle, the cycle efficiency in a recuperated cycle decreases with decreases in turbo-machinery efficiencies but this drop is significantly less in the recuperated Brayton cycle. The efficiency of the recuperated Brayton cycle is strongly dependent on the recuperator effectiveness. The greater the effectiveness, the less heat is required to attain the turbine inlet temperature and the more working fluid, hence more net output, will result. For ideal fluids, the recuperator effectiveness depends only on pressure ratio but for CO_2, there is a strong dependence on system pressure as well due to the large increase in c_p in the region of the critical point. Because of this, the recuperated Brayton cycle dependence on turbine exit pressure is complex and the maximum cycle efficiencies occur at low system pressures. However, the specific power for low system pressures is probably too low for this to be a desired operating point.

The adverse effect of low recuperator effectiveness when the CO_2 recuperated Brayton cycle operates near the critical point at the compressor entrance can be ameliorated by the use of the

two-stage recompression cycle configuration. Here, a portion of the low pressure CO_2 exiting the recuperator bypasses the CO_2 cooler and enters a second compressor directly. Only the CO_2 that has been cooled enters the low temperature recuperator stage on the cold-side. The cold-side exit stream from the low temperature recuperator stage mixes with the bypassed CO_2 and the combined stream becomes the cold-side fluid for the high temperature recuperator stage. This bypass action lowers the thermal capacitance of the cold-side fluid to be closer to the thermal capacitance of the hot-side fluid increasing recuperator effectiveness. Although this results in an increase in the compressor work, this is compensated for by the benefits of greater recuperation and greater net cycle output. The recompression configuration boosts efficiency of the recuperated CO_2 cycle, particularly at low pressure ratios where the maximum cycle efficiency occurs. As with the non-recuperated Brayton cycle, the recompression CO_2 Brayton cycle efficiency has a maximum in cycle efficiency at a turbine exit pressure just above the critical pressure. However, it is unclear if the most desired operating state for this cycle occurs at the point of maximum cycle efficiency as the specific power is quite low in this region.

The use of reheat in the recompression Brayton cycle yields an increase in both cycle efficiency and specific power although this increase is greatest at large pressure ratios. Reheat also decreases the sensitivity of the cycle efficiency to pressure ratio.

8 Recommendations

In addition to the sensitivity analyses completed in this study, additional cycle dependencies should be examined. Particularly, the dependence of the cycle performance to cooler temperature, minimum temperature approach, and pressure drop should be explored. The latter is very important in the recuperated Brayton cycle and particularly so for the recompression cycle. The recuperated and recompression cycle efficiencies show a strong dependence on pressure ratio and would be expected to be very dependent on the cycle pressure drop.

The next phase of this work should examine the performance of the cycle for real heat sources. For this study, the hot source was able to transfer 100 MMBtu/hr to the working fluid regardless of the turbine inlet temperature. This may be a reasonable representation for the hot source in certain solar and nuclear energy applications; it is not an acceptable representation of fossil fuel heat sources that have extremely wide temperature ranges. As was demonstrated, for recuperated Brayton cycles, cycle efficiency increases with turbine inlet temperature and recuperator effectiveness. However, increasing the turbine inlet temperature and the recuperator effectiveness will both act to reduce the fraction of the available heat that can used in the cycle. These effects may mean that the recompression Brayton cycle needs to be incorporated into a combined cycle configuration.

As the analysis of the recompression CO_2 Brayton cycle focuses on more realistic and practical applications, systems studies should be performed to compare it to commercially available alternatives such as subcritical and supercritical steam cycles. Because of the significantly lower technology readiness level of the recompression CO_2 cycle, estimates for appropriate operating conditions and estimates for loss terms will be more uncertain than for the very mature steam cycles. Hence, any system study comparing the implementation of these cycles should include sensitivity analyses on the key operating conditions and sources of losses.

The results of this study suggest that attempts to optimize the performance of the recompression CO_2 Brayton cycle need to factor in cost in the analysis. A number of sensitivity runs for this study showed that operating the cycle at peak efficiency may lead to very low values for specific power. It is recommended that the next phase of this work include additional cost surrogate variables. However, an optimum operating state cannot be reliably identified without a detailed design and accompanying engineering and materials selections allowing an accurate cost estimate.

9 References

1. **National Energy Technology Laboratory.** *Supercritical CO2 Power Cycles Literature Survey.* [Unpublished report] s.l. : Prepared by John Brewer, December 2012.

2. —. *Supercritical CO2 Power Cycles - Critique of Pratt & Whitney Rocketdyne Process.* [Unpublished report] s.l. : Prepared by Amy Maples and Charles White, August 2013.

3. **Shepherd, D. G.** *Principles of Turbomachinery.* NY : Macmillan Publishing Co., Inc, 1989.

Wally Shelton
Walter.Shelton@netl.doe.gov

Mark Woods
Mark.Woods@contr.netl.doe.gov

www.netl.doe.gov
Pittsburgh, PA • Morgantown, WV • Albany, OR • Sugar Land, TX • Anchorage, AK
(800) 553-7681